

Hydrothermal Treatment of Low Rank Coal for Making High Solid Loading
and Stable Coal Water Slurries

by

Qiang Li

A thesis submitted in partial fulfillment of the requirements for the degree of

Master of Science

in

Chemical Engineering

Department of Chemical and Materials Engineering
University of Alberta

© Qiang Li, 2014

ABSTRACT

The objective of this research is to understand the effect of hydrothermal dewatering (HTD) on surface properties, stability and rheological behavior of lignite water slurry (LWS). The surface forces between coal particles are found to be attractive after HTD, which is proven by contact angle and zeta potential measurement, FTIR characterizations, and modeling using extended DLVO theory. The attractive particle network could be formed in highly concentrated slurry to increase LWS stability after HTD as shown by stability measurements. The rheological studies show that HTD treated LWS exhibits lower shear viscosity at 100 s^{-1} than raw LWS at the same mass fraction, which is probably attributed to the decrease of effective volume of HTD coal particle caused by the permanent reduction of both bound and non-freezable water in lignite. The maximum lignite concentration can reach 62 wt % by HTD at 300 °C and adding 1.0 w t% db (dry base) of polycarboxylate ether (PCE).

To the one I love

ACKNOWLEDGEMENT

I would like to express my sincere gratitude to my supervisors Prof. Qingxia Liu for the continuous support of my study and research. I wish to thank Dr. Dingzheng Yang for his valuable discussion. I also thanks Prof. Hongbo Zeng, Prof. Rajender Gupta and Prof. Zhenghe Xu for letting me use the equipment in their lab. My gratitude also extends to Dr. Moshfiqur Rahman, Mohammad Sharifi, Dr. Zhenzhen Lu, Dr. Ruichi Chu, Dr. Jiantao Zhao, Dr. Haijun Zhang, Zhaohui Qiu, Erin Furnell and Patricia Siferd for their help. I would also like to thank all members of Canadian Centre for Clean Coal/Carbon and Mineral Processing Technologies (C⁵MPT) and the staff in the Department of Chemical and Materials Engineering for their kind assistance throughout my graduate studies. I also thank my parents and the one I love, but finally left, for their unceasing encouragement and support.

Table of Content

1	Introduction.....	1
	1.1 Background.....	1
	1.2 Thesis outline.....	3
2	Literature Review.....	5
	2.1 Coal dewatering method.....	5
	2.1.1 Comparison of different dewatering technologies.....	5
	2.1.2 Hydrothermal dewatering (HTD).....	9
	2.2 Rheology and stability of coal water slurry (CWS).....	10
	2.2.1 Coal water slurry.....	10
	2.2.2 Physicochemical properties.....	12
	2.2.3 Volume fraction.....	13
	2.2.4 Particle size and particle size distribution (PSD).....	14
	2.2.5 Interparticle forces.....	17
	2.2.6 Rheology of CWS.....	20
	2.2.7 Stability.....	22
	2.3 Slurryability of lignite and dewatered coals.....	23
	2.3.1 Coal water slurry made by low rank coal.....	24
	2.3.2 Coal water slurry made by dewatered low rank coal.....	24
3	Experiment Setup.....	27
	3.1 Materials.....	27
	3.2 Raw and dewatered coal analysis.....	28

3.2.1	Coal particle size distribution measurement	28
3.2.2	Coal density measurement	30
3.3	Hydrothermal treatment	30
3.4	Downstream treatment	31
3.4.1	Filtration and vacuum oven drying	31
3.4.2	Slurry making.....	32
3.5	Coal surface characterization	32
3.5.1	Contact angle and penetration time.....	32
3.5.2	Diffuse reflectance infrared Fourier transform spectroscopy (DRIFTS)	33
3.5.3	Zeta potential measurement	33
3.6	Coal structure characterization	33
3.6.1	Equilibrium moisture	33
3.6.2	Differential scanning calorimeter (DSC).....	34
3.7	Stability measurement.....	34
3.7.1	Glass rod penetration test.....	34
3.7.2	Mud line measurement.....	35
3.8	Rheology	36
4	The Effects of Hydrothermal Treatment on Bulk and Surface Properties of Lignite.....	38
4.1	Proximate analysis of raw and dewatered coal	38
4.1.1	Proximate analysis of coal samples treated at different HTD temperature	38

4.1.2 Proximate analysis of raw and HTD coal with different particle size	39
4.2 Water in coal	40
4.2.1 Desiccator method	40
4.2.2 Differential scanning calorimetry (DSC) method.....	41
4.3 Surface properties	45
4.3.1 Contact angle	45
4.3.2 Oxygen functional group	46
4.3.3 Zeta potential	47
5 The Effects of Hydrothermal Treatment on the Stability of Lignite Water Slurry.....	49
5.1 Interaction between particles modeled by extended DLVO theory	49
5.2 Stability.....	52
5.3 Yield stress and fractal dimension	55
6 The Effects of Hydrothermal Treatment on the Rheological Behaviors of Lignite Water Slurry	59
6.1 Measurement.....	59
6.2 Particle size distribution.....	62
6.3 Hydrothermal treatment temperature	63
6.4 Fines in CWS	67
6.5 Volume fraction and modeling	68
6.6 Dispersant	72
7. Conclusions.....	78
8. Contribution to Original Knowledge	81

9. Future Work	82
References	83
Appendix.....	89
A.1 Energy balance of HTD and comparison with thermal drying.....	89
A.2 Calculation of PCE volume percent.....	93

List of Tables

Table 2.1 Comparison of different dewatering technologies	6
Table 2.2 Fuel energy densities	11
Table 4.1 Proximate analysis of BD lignite and HTD products	39
Table 4.2 Proximate analysis of grinded raw BD coal	40
Table 4.3 Proximate analysis of hydrothermal treated BD coal (300 °C)	40
Table 4.4 Summary of DSC results	45
Table 5.1 The values of parameters for calculation	51
Table A.1 Parameters used for calculation.....	90
Table A.2 Parameters and values for PCE volume percent calculation.....	93

List of Figures

Figure 1.1 Percentage of lignite reserves in world total coal reserves.....	2
Figure 2.1 Schematic representation of monosized and polysized particles.	16
Figure 2.2 Effect of PSD mixture model on viscosity	17
Figure 2.3 Particle–particle interaction potential energy	19
Figure 2.4 Rheogram of various flow behaviors	21
Figure 2.5 Illustration of concentrated suspensions.....	23
Figure 3.1 Grinder and sieves	28
Figure 3.2 Particle size distribution of raw BD coal.....	29
Figure 3.3 Particle size distribution of raw BD 106-150 with and without fines.....	29
Figure 3.4 Hydrothermal dewatering autoclave.....	31
Figure 3.5 Schematic graph of coal water slurry in cylinder after storage ...	36
Figure 4.1 Equilibrium moisture of BD coal and its HTD products at different HTD temperature (at 96 % relative vapor pressure and 30 °C)	41
Figure 4.2 (a) DSC thermographs and (b) the water congelation heat of BD300 samples	44
Figure 4.3 Contact angle of raw and HTD BD coal samples.....	46
Figure 4.4 FTIR spectra of raw and HTD BD coal at 70 °C	47
Figure 4.5 Zeta potential of hydrothermal treated sample at natural pH (7.2 - 8.2)	48
Figure 5.1 Potential energy curves of two coal particles as a function of their distance modeled by extend DLVO theory.....	52

Figure 5.2 Effect of storage time on stability of CWS indicated by penetration ratio	54
Figure 5.3 Effect of storage time on stability of CWS indicated by separation ratio	54
Figure 5.4 Effect of hydrothermal dewatering temperature on the shear stress at different shear rate (samples are all at 45 wt% db).....	56
Figure 5.5 Yield stress in relation with volume fraction.....	58
Figure 6.1 Effect of thixotropy on viscosity (sample of BD300 38-75 55wt% db)	61
Figure 6.2 Effect of pre-shear on the viscosity (sample of BD300 38-75 55wt% db).....	62
Figure 6.3 Effect of the bimodal particle size distribution on the viscosity of lignite water slurries (58 wt% db total solid loading, mixture combines BD300 38-75 with BD 106-150, 100 s ⁻¹ shear rate)	63
Figure 6.4 Effect of HTD temperature on the viscosity of lignite water slurry. (a) Flow curves at various HTD temperatures; (b) Viscosity at 100 s ⁻¹ shear rate versus HTD temperature (45 wt% db lignite water slurry) ..	66
Figure 6.5 Effect of fines on the viscosity of CWS	68
Figure 6.6 Conversion of solid loading to volume fraction and the relation with relative viscosity	71
Figure 6.7 Effect of volume fraction on the relative viscosity of raw and HTD lignite water slurry.....	72
Figure 1.1 Illustrations on the interactions between different coal particles and PCE molecules.....	75
Figure 6.9 Effect of dispersant concentration on the viscosity of coal water slurries. (Sample: BD300 slurry 58 wt% db, BD raw slurry 48 wt% db, pH= 7.5 ± 0.5).....	76

Figure 6.10 Effect of hydrothermal treatment, particle size distribution and dispersant on the viscosity of lignite water slurry (shear rate 100 s^{-1}).. 77

Figure A.1 Comparison of HTD and thermal drying at different initial water contents in coal samples..... 92

List of Symbols

ASTM: American Society for Testing and Materials

BD coal: Boundary Dam coal

BD300: sample of BD coal hydrothermally treated at 300 °C

CWS: Coal Water Slurry

daf: dry, ash-free basis

db: dry basis

DLVO: Derjaguin–Landua–Verwey–Overbeek

DRIFTS: Diffuse Reflectance Infrared Fourier Transform Spectroscopy

DSC: Differential Scanning Calorimeter

EDL: Electrical Double Layer

FTIR: Fourier Transform Infrared Radiation

HTD: Hydrothermal Dewatering

HTT: Hydrothermal Treatment

LRC: Low Rank Coal

LWS: Lignite Water Slurry

MWD: Microwave drying

PCE: Polycarboxylate Ether

PSD: Particle Size Distribution

MTE: Mechanical Thermal Expression

SFBD: Steam fluidized bed drying

VDL: Van der Waals

WTA: fluidized bed drying with internal heat recovery

1 INTRODUCTION

1.1 BACKGROUND

Coal, a common source of fossil fuel, plays an important role in the world's energy. About 27 % of the total energy consumption in the world is from coal, meanwhile coal is also the largest source of fossil fuel for the power generation of electricity worldwide [1]. Canada has approximately 6.5 billion tones of recoverable coal reserves which are around 1% of the world total [2]. British Columbia, Alberta, and Saskatchewan have the largest reserves in Canada that are actively mined. As showed in Figure 1.1, 23% of the world's coal reserves are estimated to be lignite [2]. However, lignite as a low rank coal contains high moisture, so an extra 7-10 % of fuel is consumed in order to evaporate the moisture in the boiler [3]. Moreover, the high moisture content makes it uneconomic to transport lignite over long distances, and precautions are needed during storage and transportation to prevent the spontaneous combustion.

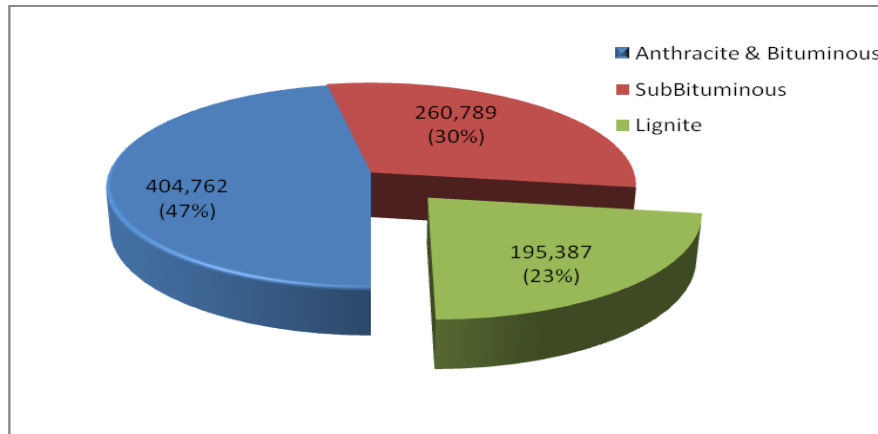


Figure 1.1 Percentage of lignite reserves in world total coal reserves [1]

Various dewatering and upgrading processes have been developed since 1920s to produce coal with high heat value and low transportation cost [4,5]. Four major dewatering technologies are:

- Mechanical thermal expression (MTE)
- Hydrothermal dewatering (HTD)
- Steam fluidized bed drying (SFBD)
- Microwave drying (MWD)

Dewatering technologies aim to remove water from coal with different mechanisms. The water removal mechanisms can be generally classified into four categories: thermal, hydrothermal, compression and microwave. Traditional dewatering or drying methods, such as thermal drying, only remove the water in the lignite temporarily without reducing the hydrophilic surface and the pore volume where the moisture is held [6]. It is difficult to transport lignite, even the dewatered lignite due to the moisture re-absorption. Therefore, the main application of dewatered lignite is direct combustion.

Currently the low rank coal water slurry (CWS) has a relatively low heat value compared with those made by high rank coal, so it is lack of commercial attraction [7, 8]. Even after traditional drying, low rank coal is easy to reabsorb water in the slurry to lower the solid concentration of the slurry. Hydrothermal treatment/dewatering (HTD) is a promising method to remove water from low rank coal to make high solid loading slurries [9, 10]. Different from traditional drying, HTD can efficiently prevent moisture from reabsorption by reducing the inherent moisture permanently and by making the lignite surface hydrophobic [9]. Therefore a high-performance CWS with high solid loading and stability can be achieved after HTD. However, the effect of HTD on the stability and rheology of the hydrothermally treated lignite water slurry are less researched. There is a need to investigate the mechanism of hydrothermal dewatering and the effects of HTD on the stability and rheological behavior of lignite water slurry.

1.2 THESIS OUTLINE

This thesis has been divided into five chapters:

Chapter one: This chapter gives a general introduction on lignite dewatering and slurry making, as well as the thesis outline.

Chapter two: This chapter provides a review on the lignite dewatering methods, rheology and stability of coal water slurry, and slurryability of raw and dewatered lignite.

Chapter three: This chapter describes the materials and methods that were used throughout the study. Equipment operational procedures were described in addition to sample preparation.

Chapter four: This chapter shows the results and discussion about the effects of hydrothermal treatment on the surface and bulk properties of lignite.

Chapter five: This chapter shows the results and discussion about the effects of hydrothermal treatment on stability of coal water slurry.

Chapter six: This chapter shows the results and discussion about the effects of hydrothermal treatment on the rheological behavior of coal water slurry.

Chapter seven: This chapter summarizes the major findings of the project.

Chapter eight: This chapter states the contribution to original knowledge.

Chapter nine: This chapter makes suggestions for the future work.

The references and appendix are shown at last.

2 LITERATURE REVIEW

2.1 COAL DEWATERING METHODS

2.1.1 Comparison of different dewatering technologies

Since 1920s, many dewatering and upgrading methods for low rank coal have been developed. The comparison of different dewatering or drying technologies is listed in Table 2.1. For making high solid loading and stable water slurry, hydrothermal treatment/dewatering (HTD) has its own advantages over others:

1. The final product is directly slurry;
2. The dewatered coal particles are stable in water environment without moisture re-adsorption.
3. HTD can be industrialized into a continuous process by Exergen CHTD technology [11].
4. HTD can be directly connected to gasifier, such as GE gasifier, and save the heat and pressure of whole system.
5. HTD is more energy-efficient than traditional drying, such as thermal drying. The energy balances of both HTD and thermal drying process are demonstrated in the Appendix A.1.

Table 2.1 Comparison of different dewatering technologies [11, 12, 13]

Option	MTE	HTD	WTA	MWD
Process description	Mechanical thermal expression (MTE) involves squeezing the water out of the lignite using mechanical energy, typically at 5 - 25 MPa pressure and temperatures in the range of 150 - 200 °C, and the vessel pressure is generated autogenously, so that water remains in the liquid state and is not evaporated.	Hydrothermal dewatering (HTD) or hot water washing is a non-evaporative drying process. Water is removed as a liquid from coal in an autoclave at typically 300 °C and 100 Bar.	Fluidized bed drying with internal heat recovery (WTA) works according to the principle of a stationary fluidized bed with low expansion. The energy needed for drying is injected via heat exchangers, which is integrated into the fluidized-bed dryer and heated with steam.	Microwave dewatering (MWD) uses microwave to drying coal and usually control the temperature below 105 °C, and usually in a continuous process.
Coal Output Moisture Level	<18%	<15%	<14%	< 12%

Advantages	<p>Latent heat of vaporization is saved, thus increase efficiency and reduce CO₂ emission</p> <p>Relative low operate temperature (at 150 - 200 °C compares to HTD) and relative low pressure (at 6 MPa compares to normal mechanical expression)</p> <p>Low reabsorb water due to irreversible pore collapse after treatment</p> <p>Reduction of mineral content</p>	<p>Latent heat of vaporization is saved, thus increase efficiency and reduce CO₂ emission</p> <p>HTD products were more hydrophobic, thus easily making slurry than original coal and prompt flotation performance</p> <p>Low reabsorb water due to irreversible pore collapse after treatment</p> <p>Reduction of inorganic content</p>	<p>Drying at low temperature thus given a high energy efficiency and energetic use of the evaporated coal water, also reduce CO₂ emission up to 30 - 40% (via mechanical vapor recompression or vapor condensation for preheating)</p> <p>High drying capacity per dryer unit</p> <p>Drying in an inert atmosphere, which makes relative safe in operations</p>	<p>Volumetric heating and heat water directly with less energy loss on the bulk carbon</p> <p>Faster drying rate, thus short residence time</p> <p>Reduction of impurities such as sulfur, potassium and phosphorous</p> <p>Do not need water during treatment</p>
------------	----------------------------------------------------------------------------------------------------------------------------------------------------------------------------------------------------------------------------------------------------------------------------------------------------------------------------------------------------------------------------------	-----------------------------------------------------------------------------------------------------------------------------------------------------------------------------------------------------------------------------------------------------------------------------------------------------------------------------------------------------	----------------------------------------------------------------------------------------------------------------------------------------------------------------------------------------------------------------------------------------------------------------------------------------------------------------------------------------------------------------------------	--------------------------------------------------------------------------------------------------------------------------------------------------------------------------------------------------------------------------------------------------------------------

Disadvantages	<p>Waste water treatment (partly reduced by novel MTE approach)</p> <p>Long residence times (but already be overcome by novel MTE approach)</p>	<p>Slurry preparation are needed</p> <p>Waste water treatment</p>	Direct to boiler only, haven't developed other downstream usage.	<p>Relative high capital and operating costs</p> <p>Hard to keep heating coal uniformly or evenly</p> <p>Potential fire hazard during drying</p>
Industry Maturity	<p>The CRC (Cooperative Research Centre) had developed a laboratory scale continuous MTE process, a 1 t/h pilot plant and a 15 t/h demonstration unit (Australia).</p> <p>In Germany, RWE Energies successfully operated a MTE demonstration plant with an output of 15 tons of dry brown coal per hour in 2001 at the Niederaussem power station</p>	<p>Pilot Plant tests at 1m³ coal slurry/hour in Victoria and Japan</p> <p>CHTD (continuous Hydrothermal dewatering) technology developed by Exergen, has not been commercialized yet</p>	<p>Several commercial WTA plants have built or planned to build in Germany and Australia</p> <p>In Niederaussem, a raw lignite 170t/h plant has built with Coarse-grain drying with integrated vapor compression.</p> <p>In Hazelwood (Australia/planned), a raw lignite 140 t/hr. plant is planned to build with Fine-grain drying without vapor utilization</p>	<p>The initial MW drying plant of 15 t/h has operated commercially</p> <p>The second, 50 t/hr. plant was commissioned in 2007</p>

2.1.2 Hydrothermal dewatering (HTD)

Hydrothermal dewatering/treatment (HTD) is a non-evaporative drying process for upgrading lignite with high moisture content. Generally, during the HTD procedure dense lignite water slurry is sealed in an autoclave to heat up to about 300 - 320 °C at the pressure of around 100 bar. The dewatered coal sample, which is resistant to moisture re-absorption, can be gained after filtration and air drying. The concept of HTD was derived from the Fleissner process which was developed in Austria in the late 1920s and patented in 1927 and 1928 [4, 5]. The Fleissner process uses steam to heat coarse lumps of lignite in an autoclave between 180 and 240 °C to produce an upgraded hard lump fuel. This process can suppress spontaneous combustion and remove moisture partly as liquid water to save energy, but it is only useful for lump coal. A similar process was patented by Evans and Siemon in 1970 and 1971, in which 75% of the moisture in lignite was removed as liquid at temperature above 250 °C with a high pressure [14-16]. This process could be applied to lump, granular or lignite slurry mixtures.

The classic HTD mechanism was proposed by Murray and Evens (1972) [17]. The removal of liquid water during HTD is initiated by a disruption of coal-water interactions by the thermal decomposition of oxygen functional groups to H₂O, CO or CO₂. The process is completed by removal of water and evolving of carbon dioxide, and meanwhile changing surface wettability and shrinking lignite.

Murray and Evans indicated that pressure might serve nothing but to prevent evaporation, which saved energy [17].

The main advantage of the HTD process is to save energy by removing the moisture of lignite in liquid state rather than gaseous state at high pressure. Other advantages include: the water-soluble inorganics are removed with the water, small pores collapse after HTD treatment and limited moisture re-adsorption [18]. The carboxyl and hydroxyl groups in coal can be removed in the form of H₂O, CO or CO₂ through pyrolysis. This process increases the hydrophobicity of the coal surface and improves the separation of ash and coal by flotation [19]. Also, the viscosity of coal-solvent slurry (33 wt%) prepared from HTD (350 °C) was less than 1/10 of that prepared from a just dewatered coal, as claimed by Inoue et al. (2012) [20]. Therefore, hydrothermal dewatering will not only increase the space-time yield, namely the yield of the time necessary to process one reactor volume of fluid, but also suppress the scale formation of the lignite liquefaction process.

2.2 RHEOLOGY AND STABILITY OF COAL WATER SLURRY (CWS)

2.2.1 Coal water slurry

Coal water slurry (CWS or coal water slurry fuel or coal water fuel) is a fuel which consists of fine coal particles suspended in water. Commercialized CWS usually consists of 55 - 70 % of fine dispersed coal particles. [21]

CWS can be applied as liquid fuel like heavy oil in boilers and furnaces, fuel in internal combustion engines, and recently energy feedstock for co-firing of coal fines in utility boilers. Compared to solid coal, it is convenient to handle and transport with pipeline, meanwhile retaining a high energy density, as illustrated in Table 2.2. CWS is used mainly in U.S., Russia, Japan, China, and Italy. [21]

Table 2.2 Fuel energy densities [22]

Fuel	Density(lb/gal)	Btu/lb	Btu/gal	Btu/ft³
Coal in bulk (7% moisture)	6.2–9.4	12,500	76,000–116,500	573,000–872,000
Residual oil	8.2	18,263	150,000	1,122,000
60% Coal/40% water blend	9.8	8,000	78,700	589,000
70% Coal/30% water blend	10.2	9,373	95,600	715,000

Coal slurry fuels, mainly coal water slurry and coal oil slurry, have been investigated since 19th century, but economic constraints made it unfavorable for a major energy source. The energy crisis in 1973 and 1979 [23] again propelled research and development of coal oil slurry. Since 1980, the research has centered on coal water slurry to make an oil replaceable fuel in industrial steam boilers, utility boilers, blast furnaces, process kilns, and diesel engines [24, 25]. While the stable low oil price in 1980s and 1990s retarded the development coal slurry fuel. Recently, the record-high oil prices in the beginning of 21st century attract the interest in coal slurry fuel, especially CWS which is an alternative fuel for diverse

applications and is valuable for coal transportation through a long pipeline.

The physical properties of coal slurry are extremely important in the processing of the fuel. The slurry must be stable and exhibit low viscosity in the shear rates of pumping and atomization. The flow characteristics and stability of coal water slurry depend on:

- (1) Physicochemical properties of the coal,
- (2) The volume fraction of the suspended solids,
- (3) The particle size and particle size distribution (PSD),
- (4) Interparticle interactions (affected by the nature of surface groups, pH, electrolytes, and chemical additives),
- (5) Temperature. [26, 27]

2.2.2 Physicochemical properties

Slurryability means how well a coal can make a slurry. The equilibrium moisture is one of the major parameters affecting the slurryability of a coal. In a CWS with the same volume fraction of solid, the more equilibrium moisture inside of coal, the less dry solid (or heat value) can be added into a CWS fuel. The more hydrophilic a coal is, the more water is inside of the coal. This will make less concentrated slurry in the same volume fraction. On the contrary, a hydrophobic

high rank coal can form the slurry more easily with low viscosity at high solid loading than low rank coal. However, a strong hydrophobic coal surface will make coal particle agglomerate or coagulate to a bigger particle and easy to settle down, rendering a poor stability [28, 27].

2.2.3 Volume fraction

CWSs are generally loaded with the highest possible concentration at an acceptable viscosity during the processing. The viscosity of the slurry increases with increasing solid loading or volume fraction.

In the current available rheological models relating the effect of the solid concentration, the volume fraction is more often used rather than weight fraction. The volume fraction is calculated in different ways for high and low rank coal. For high rank coal with low moisture content, the volume is calculated from dividing coal mass by its density. Therefore, the volume fraction (ϕ) for the CWS is represented by the equation below:

$$\phi = \frac{\frac{m_{\text{coal}}}{\rho_{\text{coal}}}}{\frac{m_{\text{H}_2\text{O}}}{\rho_{\text{H}_2\text{O}}} + \frac{m_{\text{coal}}}{\rho_{\text{coal}}}} \quad (2 - 1)$$

where m_{coal} and $m_{\text{H}_2\text{O}}$ are the weight of coal and water, and ρ_{coal} and $\rho_{\text{H}_2\text{O}}$ are the density of coal and water.

To obtain the volume fraction (ϕ) of low rank coal the amount of moisture should be taken into account. The following relation was proposed by Goudoulas et al. [29].

$$\phi = \frac{1 + a_{\text{hum}} \left(\frac{\rho_{\text{lignite}}}{\rho_{\text{H}_2\text{O}}} \right)}{1 + \left(\frac{\rho_{\text{lignite}}}{\rho_{\text{H}_2\text{O}}} \right) \left(\frac{m_{\text{H}_2\text{O}}}{m_{\text{lignite}}} \right)} \quad (2 - 2)$$

where a_{hum} is the equilibrium moisture which can be measured from the experiments. The maximum packing volume fraction (ϕ_m) can also be calculated using the above equation.

2.2.4 Particle size and particle size distribution (PSD)

Typical coal water slurry fuels have a particle size distribution (PSD) with 10–80% of the particles smaller than 74 μm (-200 mesh) and most of the particles are larger than 1 μm [21]. Settling is commonly observed for CWS. The settling of coal particles is a complex phenomenon, involving hydrodynamic and physiochemical effects. The Reynolds number (Re) of the settling of fine coal particle in slurry is far smaller than 1, so the Stokes' equation can be used to roughly estimate the settling velocity of a single particle.

$$v = \frac{d^2 g (\rho_1 - \rho_2)}{18\mu} f(\phi) \quad (2 - 3)$$

where

μ = viscosity of dispersing medium

ρ_1 = density of dispersed medium

ρ_2 = density of dispersing medium

d = diameter of dispersed particles

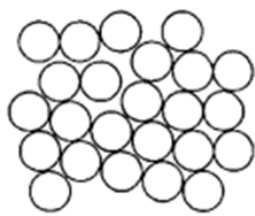
g = gravitational acceleration

$f(\phi)$ = is a function of volume fraction of suspended solids

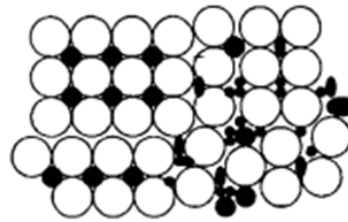
From the Stokes' equation, in order to reduce the settling velocity, the particle diameter and the difference of density between two phases should be decreased, while the viscosity of the dispersing medium should be increased. However, the transportation and atomization of CWS require a low viscosity of slurry with high solid loading.

CWS are most economical when they have the highest amount of dry coal at an acceptable viscosity. To obtain the highest possible solid loading, a bimodal or multimodal PSD is utilized, as shown in the Figure 2.1 below. The finer coal particles fit into the voids of the larger coal particles, forming a higher concentrated package of particles [31]. The unimodal coal water slurry may have a peak solid loading of ~65 wt% where the viscosity becomes infinite, whereas idealized multimodal system can generate a theoretically possible solid loading

over 80 wt% [32], as shown in Figure 2.2. The lowest viscosity of a coal-water mixture occurs usually at a fine-to-coarse ratio of $35 \pm 5: 65 \pm 5$, as stated by Barnes et al. [30]. Multimodal systems are commonly used because they are easily obtained by grinding. It should be noted that the ultrafine coal particle may act as a bridge in the intersection of relative big particles to connect other coal particles to form a network.



Monosized particles



Polysized particles

Figure 2.1 Schematic representation of monosized and polysized particle packing[31]

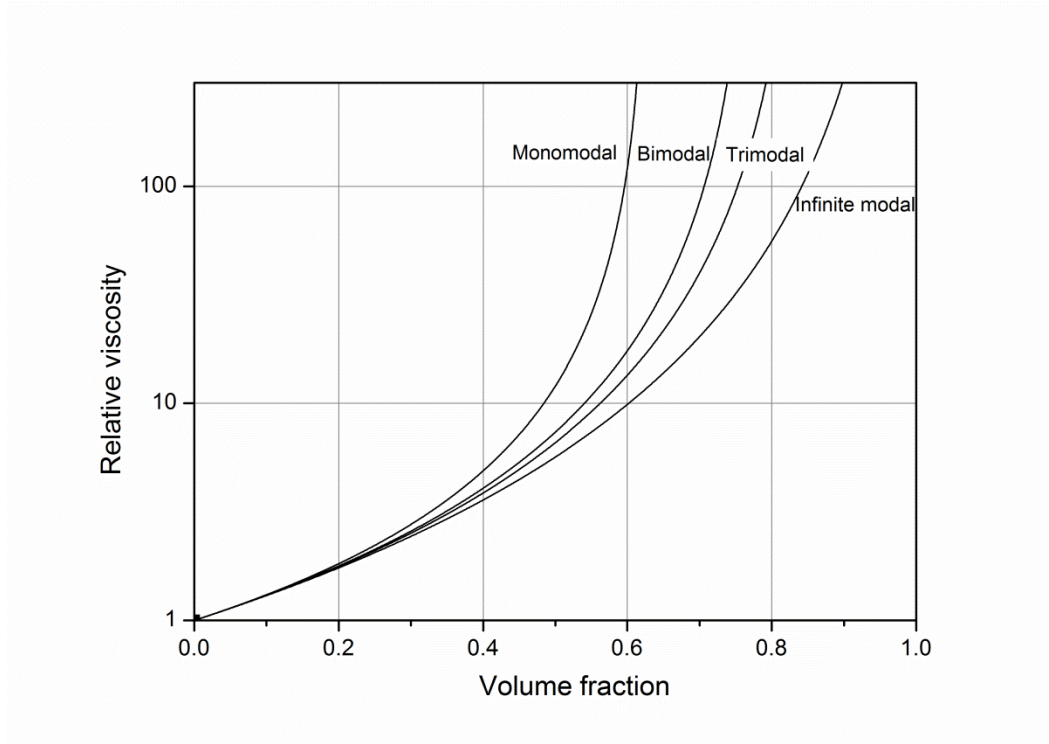


Figure 2.2 Effect of PSD mixture model on viscosity [32]

2.2.5 Interparticle forces

The forces between coal particles are one of main factors governing the rheological property of CWS. Six important particle–particle interactions may exist in aqueous dispersions as stated below [33]. More information can be found in literature [34, 35]

1. Electrical double layer (EDL) force
2. Van der Waals (VDW) attraction
3. Steric force
4. Polymer flocculation

5. Hydration- and solvation-induced force

6. Hydrophobic force

When a substance is brought into contact with an aqueous polar medium, it acquires a surface electrical charge through mechanisms such as ionization, ion adsorption, or ion dissolution. The surface charge influences the distribution of nearby ions in solution. This, coupled with thermal motion, leads to the formation of the electrical double layers (EDL). The EDL consists of a surface charge with neutralizing excess of counter-ions, and co-ions distributed in a diffuse manner [33]. In coal water slurry, the EDL forces usually play as a repulsive force, because the natural zeta potential of coal surface is negative.

Van der Waals force between coal particles in water is always attractive, which is due to the spontaneous electric and magnetic polarizations [33]. In Hamaker's method, for identical spheres, the Van der Waals force is represented by:

$$V_A = -\frac{Aa}{12h} \quad (2-4)$$

where A is the Hamaker constant, h is distance between two spheres, a is the radius of particle.

Combining the interaction of the EDL forces and Van der Waals forces, we can get:

$$V_T = V_A + V_R \quad (2-5)$$

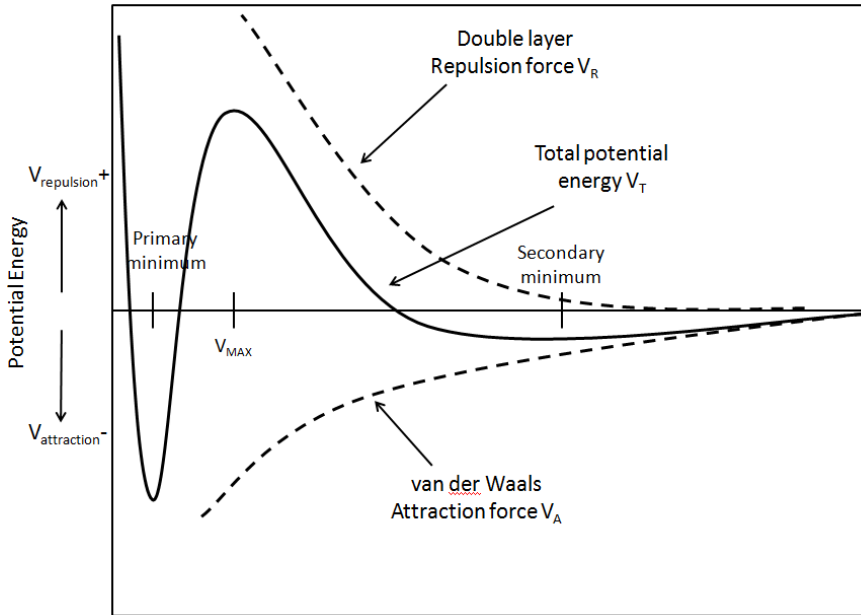


Figure 2.3 Particle-particle interaction potential energy [33]

This forms the basis of the DVLO (Derjaguin–Landua–Verwey–Overbeek) theory of colloid stability. The interaction energy caused by EDL and Van der Waals forces are shown in Figure 2.3. The total energy curve allows to predict the aggregation at the primary minimum and the possibility of a weak and reversible aggregation in the secondary minimum [36].

Steric interactions develop when molecules, usually surfactant and macromolecules, are adsorbed onto the particle surface at high coverage. When particles approach one another, part of molecules or the chain of the molecules overlap and often dehydrate to repel each other, which increases the stability of the slurry [37].

Polymer flocculation occurs when the particle surface has a relative low coverage

of high-molecular-weight polymers. The polymers bridge the particles and form flocs which might increase the viscosity and stability. [38]

Hydration- and solvation-induced interactions become important when interparticle distance is on the order of a solvent molecule. For aqueous systems, these solvation effects are clearly visible in structuring of the water near the interfacial surface, which interacts with hydrated ions from solution. When particles approach each other, it is necessary for ions to lose their bound water. Therefore, the net effect is an increased stability or net repulsion [38].

The hydrophobic forces are attractive and longer range [33]. High rank coal particles in water are easy to coagulate due to their hydrophobic surface [28].

2.2.6 Rheology of CWS

There are many definitions of rheology. One of most widely acceptable definitions is "*Rheology is the study of a system's response to a mechanical perturbation in terms of elastic deformations and viscous flow*" [39]. The type of coal, coal concentration, PSD, properties of dispersing phase, and additives are main factors that influence these responses [40].

Coal water slurry, in general, exhibits non-Newtonian behavior. However, a wide range of responses can be measured from different CWS, including Newtonian, dilatant, pseudoplastic (shear thinning), and plastic flow characteristics. Each of these flow characteristics is shown graphically in Figure 2.4.

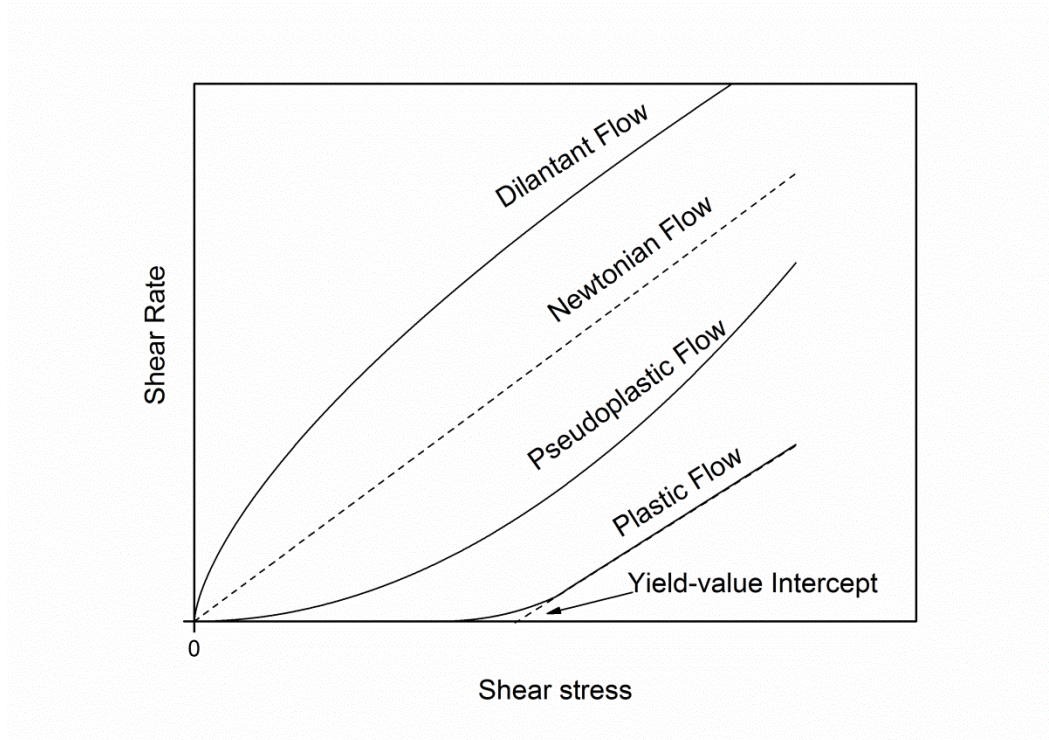


Figure 2.4 Rheogram of various flow behaviors [41]

Newtonian fluid exhibits a linear functionality between shear stress and shear rate. Pseudoplastic or shear-thinning suspension shows that as the shear stress increases, the shear rate increases at a faster rate. This behavior is caused by the breakage of the fragile internal structure or network in a suspension with increasing of shear stress. The apparent viscosity continually decreases with applied stress. [42] Thixotropy is defined as "the continuous decrease of viscosity with time when flow is applied to a sample that has been previously at rest and the subsequent recovery of viscosity in time when the flow is discontinued" [43]. Dilatant or shear thickening behavior shows that as the shear stress is increased the shear rate increases at a lower rate. In plastic behavior, a sufficient high stress must be applied to start up the flow. After the suspension yields, the shear stress is

linear with shearing rate. Viscosity, yield stress and plasticity are the important rheological characteristics. These values or properties can be determined experimentally [42].

2.2.7 Stability

The stability of a slurry can be classified into three broad categories: sedimentative (static), mechanical (dynamic), and aggregative. These three categories are crucial, according to the different applications, such as storage, transportation and atomization. Density, particle size, solid concentration, hydrophobicity, surface charge, morphology of coal, and type of medium all affect the stability of a slurry. [33]

The stability of the slurry against gravity is called sedimentative (static) stability. The statically unstable slurry will settle. In a dilute colloid system, the aggregation between particles results in a loss of stability and fast sedimentation. On the other hand, in a heavily loaded suspension with large particles ($> 1 \mu\text{m}$), like CWS, the aggregation may prevent particles from settling [44]. As illustrated in Fig. 2.5, the aggregation or flocculation creates a network of interacting or supporting particles, which could stabilize the slurry and modify the rheology of slurry [45].

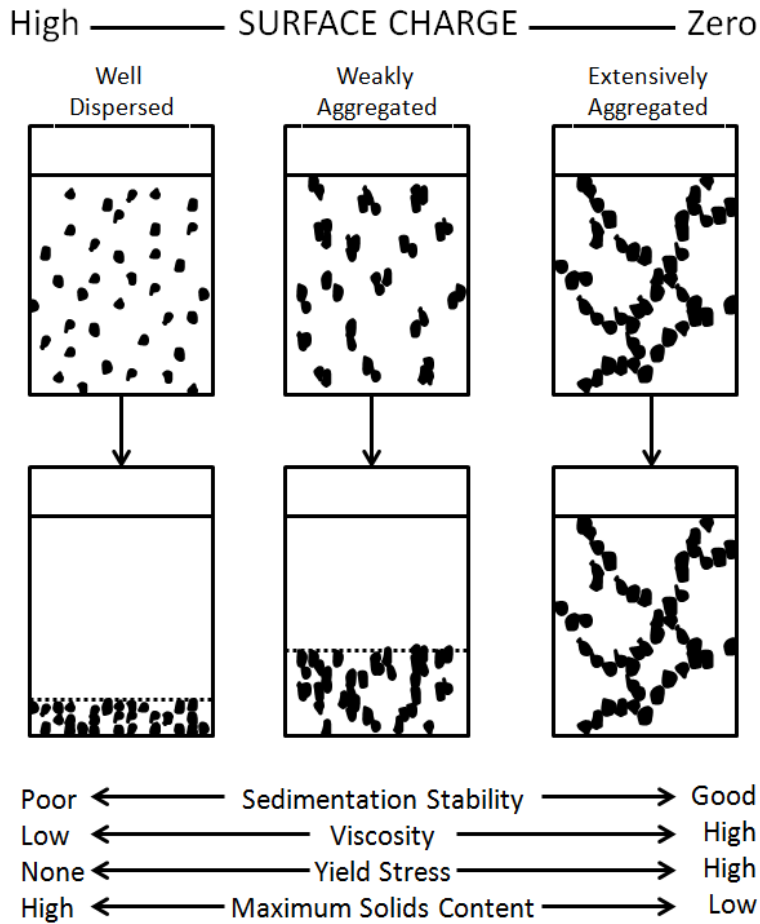


Figure 2.5 Illustration of concentrated suspensions [45]

The stability in a dynamic system is called dynamic stability. Dynamic stability involves the superposition of mechanical stresses [46]. The examples are pumping and pipeline transportation. The third stability type, aggregative stability, is a function of interparticle forces. The aggregation may increase the actual particle size, which is unfavorable in some situation, such as atomization [33].

2.3 SLURRYABILITY OF LIGNITE AND DEWATERED COALS

2.3.1 Coal water slurry made by low rank coal

Low rank coals, like lignite, usually form the slurry with a weight percentage less than 50 wt% (dry coal weight basis). On the contrary, the high-rank coals, except anthracite, could form a slurry of ~80 wt% (dry coal weight basis) [21]. However, although low rank coal water slurries have low concentrations, they have advantages of non-agglomerating and high reactivity [7].

The maximum solids concentration (ω_0) of CWS was defined as the solid concentration when the viscosity was 1000 mPa s at 20 °C. Raw lignite has the lower maximum solids concentration comparing with higher rank coal, which is probably because lots of moisture is absorbed on the surface and inside of lignite. The absorbed moisture in lignite makes it difficult on the application of combustion, gasification and other commercial usages [6, 10].

2.3.2 Coal water slurry made by dewatered low rank coal

Evaporative drying, such as traditional thermal drying and steam fluidized bed drying, can dry lignite with a low final moisture, but the product is always easy to reabsorb moisture. Lignite water slurry tends to cake or settle during a long period storage [47, 48]. In evaporative drying process, the low heating temperature can't decompose the oxygen function groups. At atmospheric pressure, tars and waxes tend to evaporate completely. Therefore, coal surface does not change much, and water can be still absorbed into the pores of the coal, leading to relatively high equilibrium moisture. The concentration of CWS and stability will be reduced when making CWS. It is reported that combining evaporative drying with tar coating process can increase solid loading and stability of CWS. However,

additional 2 - 5 wt% of tar was needed to be melt at high heating temperature (above 270 °C with superheated steam or above 270 °C combining vacuum) and coated on the coal surface, resulting in high energy consumption. [48, 49]

Viscosity is another important standard of making CWS. The viscosity of coal water slurry increases with the increase of solid concentration. The maximum solids concentration was found to increase with processing temperature and addition of proper surfactants [9, 50]. Favas et al. (2003) claimed that by hydrothermal treatment (HTD), the CWS made by lignite can reach a maximum solids concentration as high as 63.9% with adding 1 wt% sodium lignosulfonate as dispersant [9]. Guo et al. (2000) employed mechanical thermal expression (MTE) to obtain a maximum solid concentration of 60 wt% at 12 MPa and 280 °C using Loy Yang lignite [51].

A dry lignite concentration over 60 wt% can be made from both HTD and MTE method. However, for making high solid loading and stable lignite water slurry, HTD has advantages over MTE in:

1. The final product of HTD is slurry while it is coal briquette for MTE;
2. Continuous process can be made for HTD by Exergen CHTD technology [11], while it is batch or semi-continuous process for MTE;
3. HTD can recycle the heat and pressure of CWS when connecting directly to gasification process [11], while it is impossible for MTE.

The mechanism to make a high solid loading CWS by HTD, proposed by Favas et al. [9], is that the evaporative drying component brings the water together with

waxy materials out of the larger pores. Some of the waxy materials block the entrance to these large pores, resulting in a dramatic decrease in the number of large pores and smoothness of the external surface. However, the difference in the mechanism to make a high solid loading CWS by MTE, proposed by Guo et al., is that the increased slurryability by MTE process are more due to the micro-porosity destruction which is only influenced by process temperature and compression rather than the leaking of wax material [9, 51].

The mechanisms of improving slurryability by dewatering processing are still under development. More studies are needed to investigate the stability and rheology of CWS made from lignite after dewatering processing.

3 EXPERIMENT SETUP

3.1 MATERIALS

BD (Boundary Dam) coal, a type of lignite, was received from Sherritt Company (Estevan, Saskatchewan, Canada). The proximate analysis of the raw BD coal and hydrothermally treated samples was conducted in a Thermal Gravity Analyzer (LECO, model no. 701, United States), following the procedure stated in ASTM D7582-12.

Melflux 1641 (BASF, Ludwigshafen, Germany), a polycarboxylic ether (PCE), was used as the dispersant of coal water slurry. ACS analytical pure K_2SO_4 (Fisher Scientific, Canada) was used to measure the equilibrium moisture. Deionized water was used in all experiments.

250-350 g BD coal was dry ground in a 500 ml ball mill at 375 rpm for 6 minutes. . After grinding, an automatic shaker was applying to screen the grinded coal into 6 fractions of particle size: -38, +38-75, +75-106, +106-150, +150-212 and -212+250 μm . Each particle size fraction was sieved twice to make a clear a cut on each size fraction.



Figure 3.1 Grinder and sieves

3.2 RAW AND DEWATERED COAL ANALYSIS

3.2.1 Coal particle size distribution measurement

The Mastersizer 3000 laser diffraction particle size analyzer (Malvern Instruments, United Kingdom) was applied to measure the particle size. 5 - 20 wt% of coal suspension were added into the detect chamber till the turbidity ranged from 1 - 15 %. The five particle size ranges of coal particles, used for the experiments, are illustrated in Figure 3.2. Figure 3.3 is the particle size distribution used to test the effect of fines in slurry.

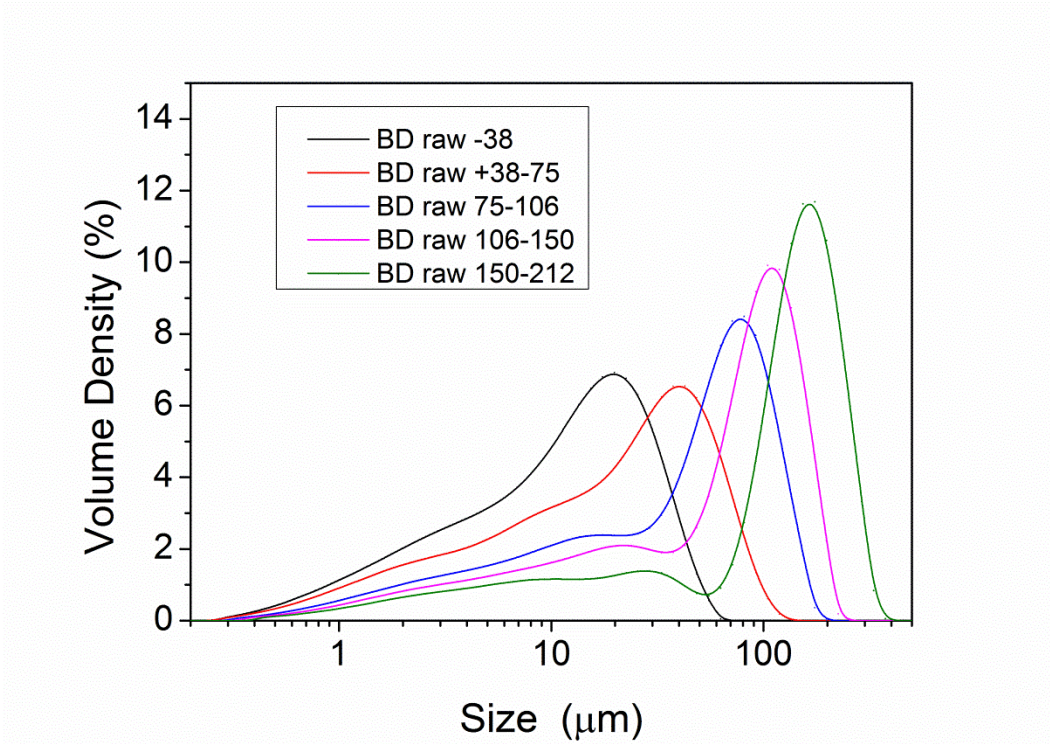


Figure 3.2 Particle size distribution of raw BD coal

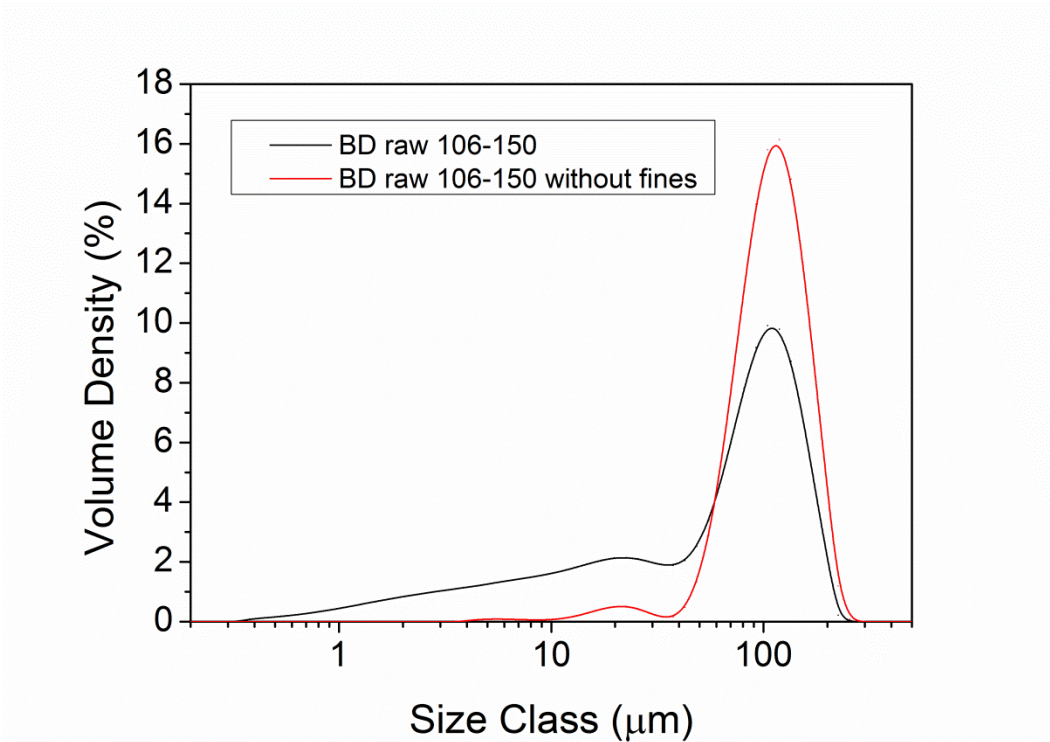


Figure 3.3 Particle size distribution of raw BD 106-150 with and without fines

3.2.2 Coal density measurement

10 g Dry coal (after drying at N₂ atmosphere for 2 hour at 105°C) was added to 50.0 ml deionized water. The density of coal sample was calculated using equation below [52]. The densities of 1.31 ± 0.05 g/cm³ and 1.53 ± 0.05 were obtained for both raw and hydrothermal dewatered (at 300 °C) lignite, respectively.

$$\text{Density} = \frac{m_{\text{dry coal}}}{V_{\text{dry coal+water}} - V_{\text{water}}} \quad (3 - 1)$$

3.3 HYDROTHERMAL TREATMENT

Hydrothermal dewatering (HTD) experiments were performed in two different autoclaves: a 500 ml autoclave (Parr-4843) and a 250 ml one (Parr-4848). The system used for hydrothermal treatment is presented in the Fig. 3.2. The autoclave was sealed and operated at 150, 200, 250, 300 and 320 °C respectively. 50 g of BD coal and 100 ml of deionized water were loaded into the autoclave reactor and purged with nitrogen until the pressure rose to 1 MPa. The slurry was then heated to the desired temperature with continuous stirring at around 350 rpm. After 20 min of reaction time, the heater was turned off and then the autoclave was cooled below 50 °C in 30 min with the cooling water. Finally, the pressure of the autoclave was released to atmosphere pressure. The obtained coal water slurry was transferred into a sealed glass jar for further tests.



Figure 3.4 Hydrothermal dewatering autoclave

3.4 DOWNSTREAM TREATMENT

3.4.1 Filtration and vacuum oven drying

The slurry was filtrated using a vacuum pump on a P2 filter paper (Fisher Scientific, Canada) retains particles above 1 μm . The residue was washed several times with deionized water and then dried in a vacuum oven at 105°C for 1.5 hours. The filtered water was collected in a glass bottle for further analysis.

3.4.2 Slurry making

After hydrothermal dewatering reaction, the CWS can be gain from the reactor. But the solid loading is too low for making a slurry over 50 wt% db. Further condensation is needed. The slurry after HTD was transferred into several centrifugal tube (50 mL bought from Fisher Scientific). The slurry was centrifuged over 7500 rpm for 30 min to separate the solid and supernate. To make a slurry with a desired dry solid loading, the associated amount of supernate was removed.

The desired amount of dispersant was added into supernate after centrifuging, the mixed with the solids in the bottom. The slurry then was stirred for at least one hour before further test.

3.5 COAL SURFACE CHARACTERIZATION

3.5.1 Contact angle and penetration time

The hydrophobicity of coal samples was determined by the contact angle measurement on a pressed fine coal disc with a drop shape analyzer (DSA 10, Krüss) equipped with an optical microscope and illumination system. The coal disc or pallet (10 mm in diameter and 4 mm in thickness) was prepared using about 350 mg of each sample (< 100 μm), pressed under high pressure (over 5500 psi) for 2 min. The sessile drop method with the drop volume of 10-20 μL was employed at the room temperature.

3.5.2 Diffuse reflectance infrared Fourier transform spectroscopy (DRIFTS)

The spectra from 400 cm^{-1} to 4000 cm^{-1} at 4 cm^{-1} resolutions was obtain by Nicolet iS50 FTIR spectrometer with a diffuse reflection accessory. A high temperature reaction chamber was attached into the diffuse reflection accessory for the in-situ measurement. About 5 mg coal sample and 50 mg analytical pure KBr powder were mixed and then loaded into the reaction chamber. The sample was heated up to $70\text{ }^{\circ}\text{C}$ with a equilibrium time of 20 min in a flowing ultra-pure nitrogen stream. Dry KBr spectrum at $70\text{ }^{\circ}\text{C}$ was used as background. The spectra obtained from the sample, deducted by the background with baseline correction, are simply called FTIR spectra here.

3.5.3 Zeta potential measurement

A suspension containing 0.05 to 0.1 wt% coal particles was prepared at its nature pH (7.2 - 8.2) with approximate 1mM NaCl. The suspension was allowed to settle 3 hours and the supernatant was used for zeta potential measurement at $25\text{ }^{\circ}\text{C}$ by employing Zetasizer Nano ZS (Malvern Instruments, United Kingdom).

3.6 COAL STRUCTURE CHARACTERIZATION

3.6.1 Equilibrium moisture

Around 3 gram coal sample (particle size $< 250\text{ }\mu\text{m}$) was put in a disc. Discs with sample were put into a desiccator. The measurement of equilibrium moisture was conducted in a desiccator with 96% relative vapour pressure (made by saturated K_2SO_4 solution), at $30\text{ }^{\circ}\text{C}$ for three days, following ASTM method [53].

3.6.2 Differential scanning calorimeter (DSC)

The moisture content of coal samples were analyzed using a TA Q1000 Differential Scanning Calorimeter (DSC) equipped with a cooling accessory (TA Instruments, United States) immediately after weighing. Typically 5-10 mg of samples were placed in the aluminum DSC sample container with pin-hole on the lid. Hydrothermally treated coal particles with different moisture contents were prepared by allowing the wet particles to lose water slowly through the pin-hole at room temperature. The sample was cooled down from 293 to 213 K at a rate of 8 K/min and then heated up to 293 K at the same rate under 50 ml/min nitrogen gas flow.

In the literature [54, 55], it was confirmed that in the range from 1 to 8 K/min, the quantity of heat evolved had a variation less than 8%. Three measurements were made by DSC on coal samples.

3.7 STABILITY MEASUREMENT

3.7.1 Glass rod penetration test

Glass rod penetration test was employed to evaluate the stability of CWS by measuring the penetration ratio (%) changing with storage time (h) as described by Qiu et al. [56].

The CWS after preparation was stored in a glass cylinder (100 mL, 18.8 cm height of calibration from 0 to 100 mL) at room temperature for a defined period.

A Schematic graph of coal water slurry in cylinder after storage is shown in Figure 3.5. A glass rod (6 mm in diameter, 30 cm in length, 27.2 g in weight) was dropped down from the CWS surface perpendicularly to the bottom of cylinder for 1 min. The glass rod stopped when the tip went through the loose lay and contacted with the hard sediment. The penetration ratio was calculated as below:

$$\text{Penetration ratio}(\%) = \frac{d_p}{d_t} \times 100 \quad (3 - 2)$$

where d_p is the distance of glass rod travel (cm), and d_t is maximum distance of glass rod can travel (cm), namely the length of slurry in cylinder.

3.7.2 Mud line measurement

The mud line is a line between the supernatant layer and dark slurry layer. The separation ratio was calculated as below:

$$\text{Separation ratio} (\%) = \frac{d_s}{d_t} \times 100 \quad (3 - 3)$$

where d_s is the length of the supernatant volume above the mud line, and d_t is the length of the total slurry volume in cylinder.

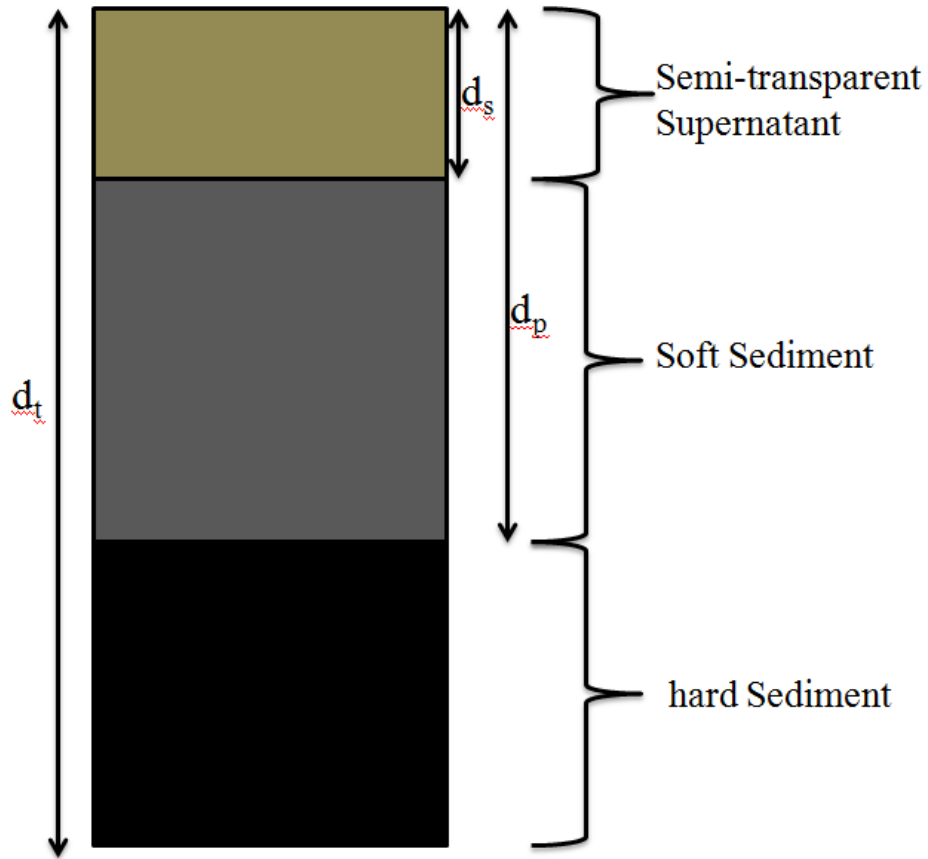


Figure 3.5 Schematic graph of coal water slurry in cylinder after storage

3.8 RHEOLOGY

The hydrothermal treated slurries were condensed into the desired solid loading for the rheological measurements through the centrifugation. One hour of mechanical mixing was applied in order to generate the homogeneous dispersions, before measurement. A stress-controlled TA DHR-2 Rheometer (TA Instruments, United States) equipped with a Peltier temperature control system was employed to measure the rheology of coal water slurries. A concentric cylinder geometry with a cup diameter of 30.41 mm and a bob diameter of 28.01 mm was selected to

minimize the segregation effect of coal particles. Prior to the measurement, a 60 seconds of pre-shear at 200 s^{-1} followed by a 30 seconds equilibrium time was applied to remove the shear history. Steady state shear sweep method was applied to measure the viscosity of coal water slurry. Proper shear rates were selected for specific samples to ensure the laminar flow. An equilibrium time of 10 seconds was used for each shear rate to make sure the steady state was reached. All the experiments were conducted at $25 \pm 0.1 \text{ }^\circ\text{C}$.

4 THE EFFECTS OF HYDROTHERMAL TREATMENT ON BULK AND SURFACE PROPERTIES OF LIGNITE

4.1 PROXIMATE ANALYSIS OF RAW AND DEWATERED COAL

4.1.1 Proximate analysis of coal samples treated at different HTD temperature

The proximate analysis of raw and hydrothermally dewatered samples are listed in Table 4.1. In these tables, "BD 150" means BD lignite hydrothermally dewatered at 150 °C and the same as other abbreviations. In Table 4.1, the sample was collected right after filtration (20 min) without further drying. With increasing the temperature of hydrothermal treatment, the moisture retaining on BD coal samples decreases after filtration. The value of fixed carbon also increases along with hydrothermal temperature. With the increase of HTD temperature, more volatile matters, a mixture of short and long chain hydrocarbons, aromatic hydrocarbons and some sulfur [57], are leached out. Little volatile matter is leached out below 150 °C, while between 150 and 250 °C, the volatile matter is slightly leached out, less than 3.1 % of total volatile matter leached out in 250 °C. When hydrothermal treatment temperature is above 250 °C, the volatile matter is leached out intensively, but still less than 10 % of total volatile matter leached out at 300 °C. In water environment, the hydrophobic volatile matter leaches into water and part of them attaches onto the coal surface, blocking the pores of the surface and making it more smooth and hydrophobic [9]. When the temperature of

HTD increases, more volatile matter will leach out in water phase and the surface of coal will become more hydrophobic.

Table 4.1 Proximate analysis of BD lignite and HTD products

Name	Moisture ^a wt%	Volatile Matter (VM) ^b wt% db	Fixed Carbon (FC) wt% db	Ash wt% db	Higher Heating Value (HHV) ^d MJ/kg
BD raw	37.06	40.77	43.57	15.66	21.64
BD 150 ^c	36.19	40.92	43.71	15.37	21.72
BD 200	36.17	40.15	44.35	15.49	21.82
BD 250	35.94	39.54	44.61	15.84	21.81
BD 300	30.44	36.08	47.60	16.32	22.33
BD 320	28.28	34.58	48.45	16.97	22.39

a. Moisture wt% : Measured after filtration on total weight percent

b. wt% db: on dry base weight percent

c. BD 150 means BD lignite HTD at 150 °C and the same as other abbreviation

d. HHV=0.3536FC+0.1559VM-0.0078ASH [58]

4.1.2 Proximate analysis of raw and HTD coal with different particle size

The proximate analysis of raw BD coal and hydrothermal treated at 300 °C with different particle size range was presented in Table 4.2 and Table 4.3. The samples of different particle size were collect right after grinding and sieving, while the samples of BD300 were collected after filtration and air-drying. In both raw and HTD samples, the moisture, volatile matter and fixed carbon increases with the increase of particle size, while ash content decreases.

Table 4.2 Proximate analysis of grinded raw BD coal

	Moisture wt%	Volatile wt% db**	Fixed C wt% db	Ash wt% db
BD212-250*	20.58	42.02	48.41	9.57
BD150-212	19.48	41.37	46.76	11.87
BD106-150	18.38	39.84	45.45	14.7
BD75-106	17.28	39.56	44.5	15.95
BD38-75	16.24	37.98	43.09	18.94
BD-38	13.57	35.55	41.66	22.78

* BD212-250 means raw BD coal passing a sieve with 250 μm open and retaining on a sieve with 212 μm open. The similar meaning for other abbreviation.

**db means dry base

Table 4.3 Proximate analysis of hydrothermal treated BD coal (300 °C)

	Moisture wt%	Volatile wt% db*	Fixed C wt% db	Ash wt% db
BD300 150-212	12.86	35.17	50.92	13.86
BD300 106-150	12.12	36.16	50.8	13.05
BD300 75-106	12.22	37.1	50.06	12.83
BD300 38-75	11.38	34.95	47.78	17.90
BD300 -38	10.88	31.33	46.64	22.09

4.2 WATER IN COAL

4.2.1 Desiccator method

In Figure 4.1, the equilibrium moisture is shown to decrease with the increase of HTD temperature. In another word a decreasing amount of water is re-absorbed into dewatered lignite with increasing HTD temperature. A dramatic decrease of the equilibrium moisture is shown at the HTD temperature from 250 to 300 °C. One reason for such phenomena is because of the reduction of the carboxylate groups after the hydrothermal dewatering, resulting in a decreased amount of water bonded onto the carboxylate groups through hydrogen bonding [17, 59]. Another reason is probably due to the sealing of pores in coal by the leached

volatile matter, which prevents water from entering into those pores [9]. In Table 4.1, it is shown that with the increase of HTD temperature the amount of volatile matter decreases with a sharp change from 250 to 300 °C.

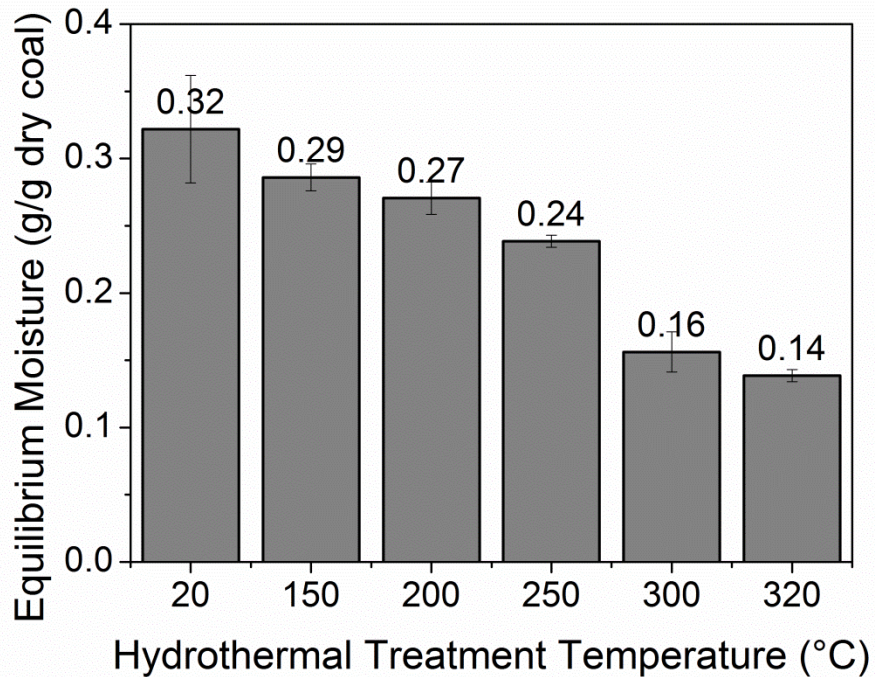


Figure 4.1 Equilibrium moisture of BD coal and its HTD products at different HTD temperature (at 96 % relative vapor pressure and 30 °C)

4.2.2 Differential scanning calorimetry (DSC) method

The water in lignite can be classified as free or bulk water, bound water and non-freezable water, according to the different freezing temperature when cooled by DSC [54]. When the lignite is dried, bulk/free water, bound water, and non-freezable water are removed successively [55]. On the contrary, during the process of water re-adsorption, a reverse sequence occurs [54, 60].

Figure 4.2(a) presents the DSC thermographs of raw and hydrothermal dewatered BD coals during the cooling from 0 to -60 °C at a rate of 8 K/min. The effect of cooling rates of 2 to 8 K/min on the thermographs on the calculated amount of different types of water was found to be negligible [54, 55]. In Fig. 3a, the peak temperature of free or bulk water is shown around -10 to -20 °C. The peak temperature of bound water is shown around -40 °C, which is probably caused by the congelation of water in capillaries with diameters less than several microns or the near layers right above coal surface [61]. The non-freezable water which is tightly bonded on the coal surface cannot freeze even at -100 °C [54, 62], so no peak of heat flow is shown.

By integrating peaks of heat flow in Fig 4.2(a), the congelation heat of both free water and bound water in coal are acquired. In Fig. 4.2 (b), congelation enthalpy as the function of water content is shown, and enthalpy-water content function is usually divided into three regimes (free water, bound water and non-freezable water) based on the slope of linear fitting of every regime [54]. The slope of linear fitting of heat-water content function at the high water content regime represents the enthalpy of free water. The congelation heat of bound water is obtained through the linear fitting of the function at medium water content as shown as the red dash line in Fig. 4.2 (b). It should be noted that the slope of non-freezable water regime is zero. The water amount at the intersection of the linear fittings of free water and bound water regimes contains both non-freezable water and bound water. The intersection of linear fitting of bound water regime with x-axis corresponds to the amount of non-freezable water. After getting the enthalpies of

free water and bound water, the amount of these water can be calculated by dividing congelation heat of water to its enthalpy. While the non-freezable water can be determined by deducting the amount of both free and bound water from total water indirectly. More details of this method can be found in [54, 55].

Table 4.4 summarized the main results of DSC method. The non-freezable and bound water can be reduced more than half of its original amount inside of coal particle by hydrothermal treatment at 300 °C. In the water slurry, the hydrothermally treated coal particle will have a higher dry solid loading, at the same volume or volume fraction.

It is noticeable that the total amount of bound and non-freezable water is slightly larger than the amount of equilibrium moisture. Compared to the equilibrium water measured at 96% relative vapor pressure, the bound water is measured next to the free water, where the relative vapor pressure is 100 %. Therefore, the value combining bound and non-freezable water should be larger than the equilibrium water (at 96% relative vapour pressure). This value can be used as inherent moisture, which is closer to the amount of water in coal when making slurry.

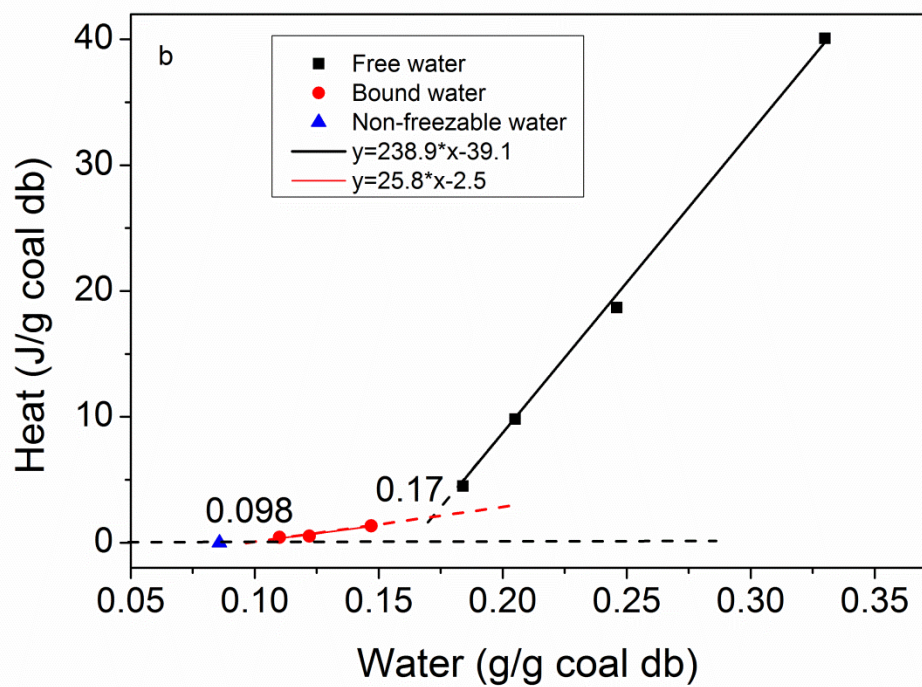
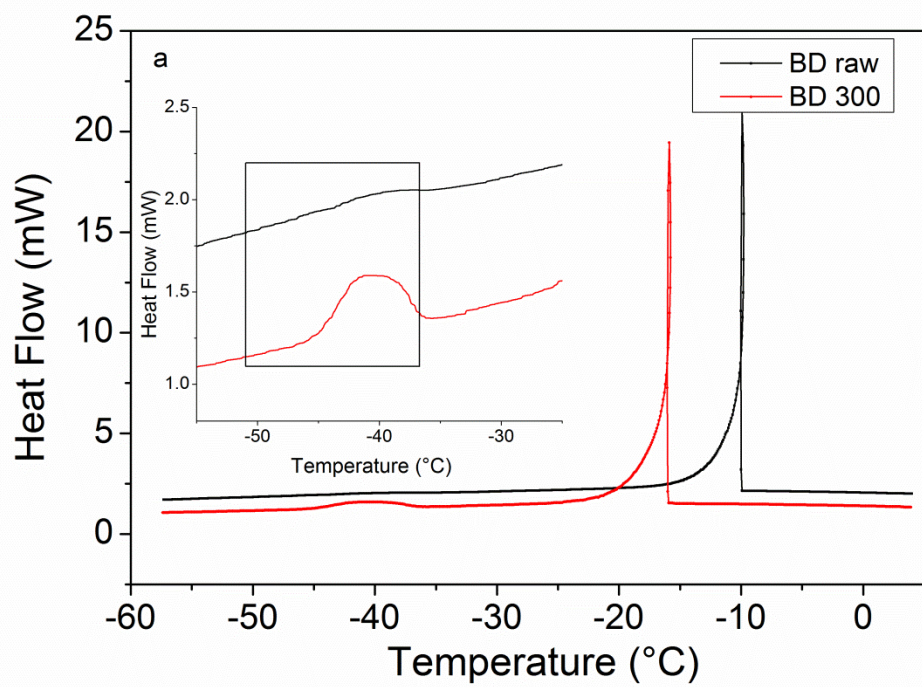


Figure 4.2 (a) DSC thermographs and (b) the water conglation heat of BD300 samples

Table 4.4 Summary of DSC results

sample	peak temperature (°C)		enthalpy of water (J/g)		water type (g/g of dry coal)		
	higher	lower	free	bound	free	bound	non-freezable
BDraw	-11	-38	255	3.83	n/a	0.16	0.23
BD300	-17	-41	239	25.8	n/a	0.072	0.1

4.3 SURFACE PROPERTIES

4.3.1 Contact angle

The contact angle of the lignite sample is directly measured on the compressed coal discs. Because the surface of coal disc is consist of both coal particle and the porous between coal particles, the value measured is different from the contact angle measured on the bulk coal surface. The contact angle measured by this method is influenced by the particle size distribution, compressing pressure, the moisture of coal and its own heterogeneity [63]. In this measurement, the particle size distribution, compress pressure, moisture of coal sample were kept at same condition. Therefore, the contact angle measured has a reliable value to illustrate the effect of hydrothermal treatment on the surface hydrophobicity.

Figure 4.3 shows that below 250 °C, the contact angle increases slightly with increasing of hydrothermal treatment temperature. When HTD is above 250 °C, the contact angle increases along with the HTD temperature, which is probably due to the leaching of volatile matter that covers the surface of lignite. In coal water slurry, increasing of surface hydrophobicity will intensify the attractive hydrophobic force between coal particles.

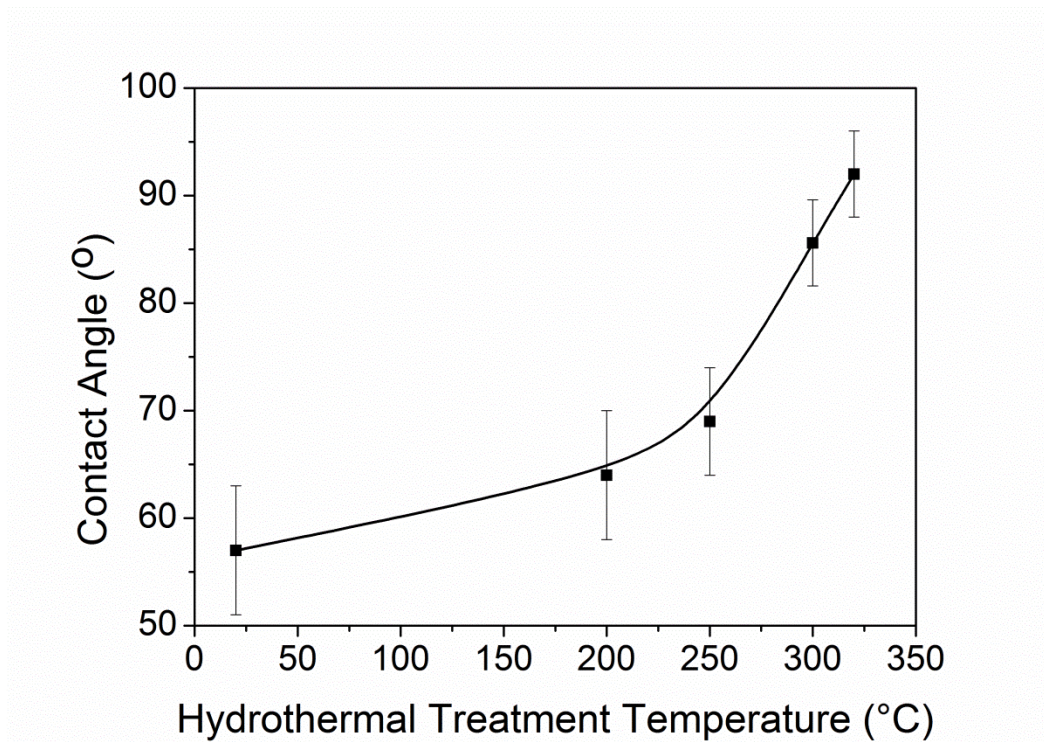


Figure 4.3 Contact angle of raw and HTD BD coal samples

4.3.2 Oxygen functional group

Figure 4.4 shows that the intensity of peaks at 3050 - 3600 and 1550 - 1650 cm^{-1} decrease with increasing the temperature of hydrothermal treatment. The peak of 3050 - 3600 cm^{-1} represents the moisture and -OH group in coal and the peak of 1550 - 1650 cm^{-1} represents the C = O and COOM groups [64]. Therefore, moisture and the oxygen functional group, such as hydroxyl and carboxyl groups, decrease with increasing the temperature of hydrothermal treatment.

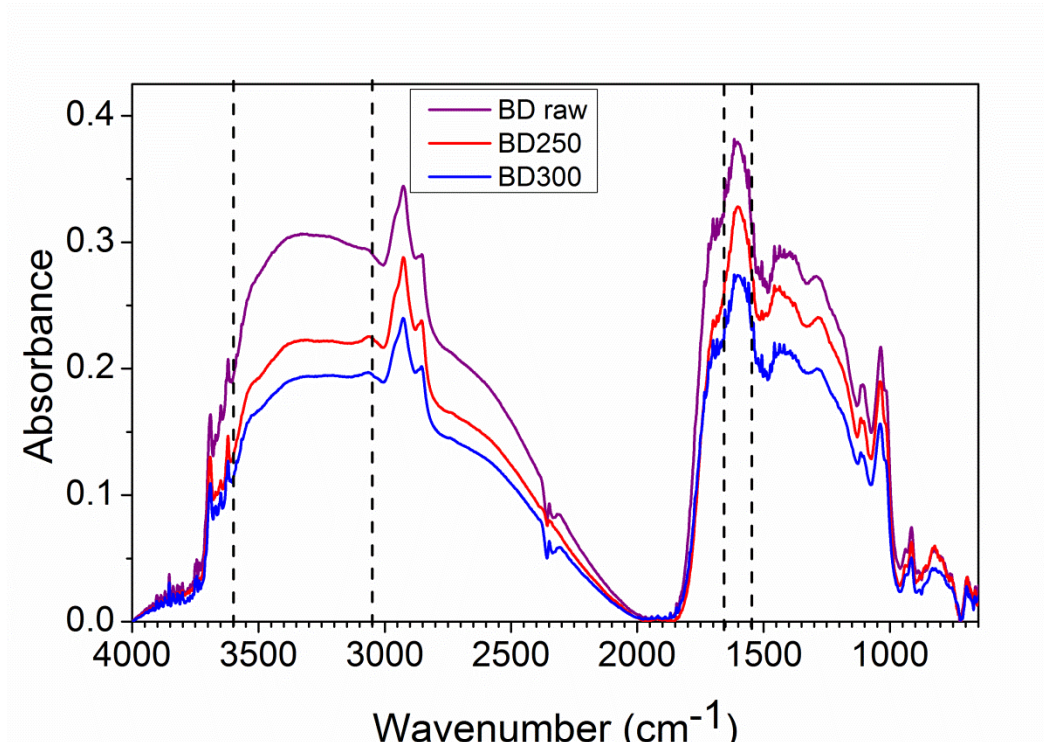


Figure 4.4 FTIR spectra of raw and HTD BD coal at 70 °C

4.3.3 Zeta potential

The zeta potential of coal is known to be negative at its neutral pH, and the value becomes less negative with the decrease of pH [50]. The zeta potential of coal surface moves towards a less negative value by increasing the temperature of hydrothermal treatment, as shown in Figure 4.5. In the temperature between 200 and 300 °C, the value of zeta potential becomes less negative quickly, while beyond this region, it did not change significantly. $-\text{COOH}$ and $-\text{OH}$ are the potential determining functional groups on the surface of the lignite [65]. Therefore, this change of zeta potential is linked with the decomposition temperature of oxygen functional group [17], as seen in Figure 4.2. A lower

absolute value of zeta potential will decrease the electrical double layer repulsion force between coal particles.

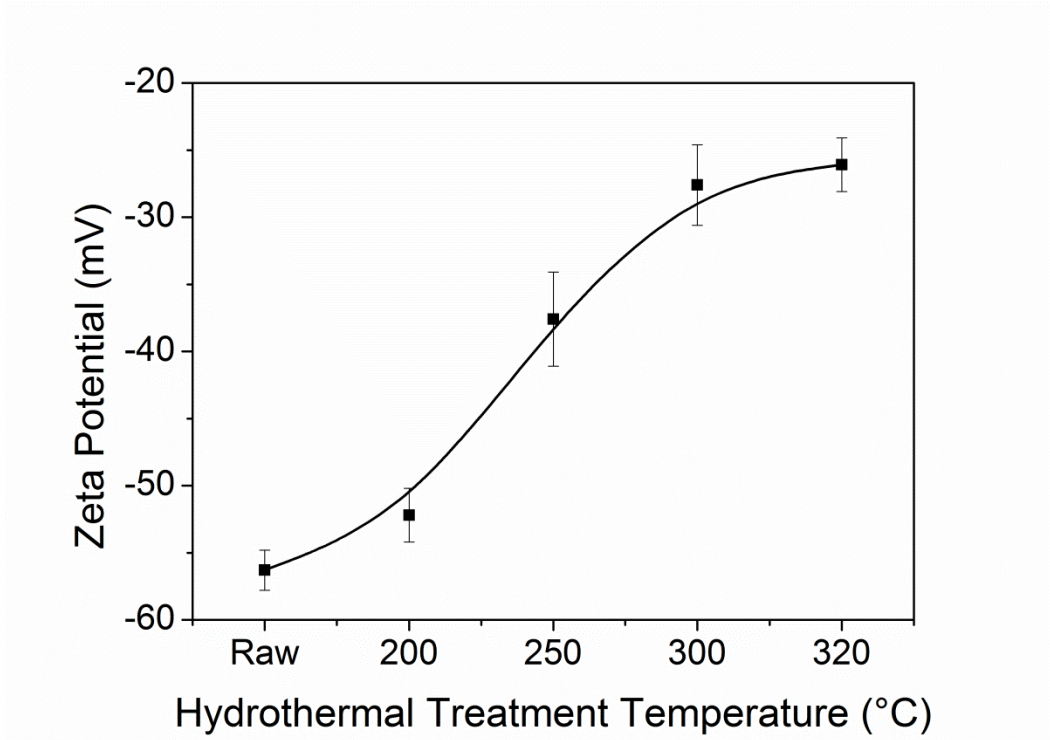


Figure 4.5 Zeta potential of hydrothermal treated sample at natural pH (7.2 - 8.2)

5 THE EFFECTS OF HYDROTHERMAL TREATMENT ON THE STABILITY OF LIGNITE WATER SLURRY

5.1 INTERACTION BETWEEN PARTICLES MODELED BY EXTENDED DLVO THEORY

The interactions between coal particles are modeled by applying extended DLVO theory [66], as shown in Equation (5-1):

$$V_T = V_D + V_E + V_H \quad (5 - 1)$$

where V_E , V_D and V_H are the potential energies due to electrostatic, Van der Waals and hydrophobic force, respectively.

For two spherical particles of radius a separated by a surface-to-surface distance H , the Van der Waals (VDW) interaction follows the expression below [67]:

$$V_D = \frac{A_{121}a}{12H} \quad (5 - 2)$$

When $a \gg H$, A_{121} is the Hamaker constant for two particles (1) acting across the medium (2). The value of Hamaker constant changes with contact angle or hydrophobicity of coal, as estimated in Table 5.1.

For two identical particles with constant surface potential (ψ_δ), electrical double layer (EDL) interaction follows the approximate expression (with error up to 40%) below [67]:

$$V_E = 2\pi\epsilon a \psi_\delta^2 \ln[1 + \exp(-\kappa H)] \quad (5 - 3)$$

where ϵ is the permittivity of the medium, κ^{-1} is the Debye screening length and ψ_δ is Stern plane potential.

For two identical spherical particles, The hydrophobic interaction follows the expression below [68, 69]:

$$V_H = -\frac{K_{121}a}{12H} \quad (5 - 4)$$

When $a \gg H$, K_{121} is the hydrophobic force constant between the two identical particles (1) in medium (2).

The hydrophobic force constant (K_{121}) can be calculated by the following expression, which is used in silica, glass and Chalcopyrite-water system [70]:

$$K_{121} = a \exp(b_k \theta) \quad (5 - 5)$$

where a and b_k are constants. When $\theta < 86.89^\circ$, $a = 2.732 \times 10^{-21}$ and $b_k = 0.04136$. [71]

Putting Equation (5-2), (5-3) and (5-4) into Equation (5-1), we can get Equation (5-6) below to calculate the potential energy between two coal particles.

$$V_T = 2\pi\epsilon a \psi_\delta^2 \ln[1 + \exp(-\kappa H)] - \frac{A_{121}a}{12H} - \frac{K_{121}a}{12H} \quad (5 - 6)$$

Table 5.1 The values of parameters for calculation [72, 73]

Sample	Zeta potential /mV	Contact Angle* (θ)/ ^o	Hamaker constant (A_{121})/J	hydrophobic force constant (K_{121})/J
BDraw	-57	50	4×10^{-20}	2.1×10^{-20}
BD250	-38	63	8×10^{-20}	3.7×10^{-20}
BD300	-28	80	16×10^{-20}	7.6×10^{-20}

* Assume the coal disc with 10% porosity on the surface

Table 5.1 shows the values of parameters in Equation (5-6). The value of ψ_δ is approximated by zeta potential from Figure 5 and the value of θ is from Figure 3. The value of A_{121} and K_{121} is estimated and calculated from the cited paper [70-73]. Increasing of HTD temperature renders a lower absolute value of zeta potential, which decreases the EDL repulsion force. Meanwhile both A_{121} and K_{121} increase with the HTD temperature, which increases the VDW attractive force and hydrophobic attractive force.

Figure 5.1 shows potential energy curve of coal particle surface changes with the temperature of hydrothermal dewatering. Increasing HTD temperature reduces the energy barrier of repulsion, and finally the energy barrier vanishes. By decreasing of EDL repulsive force and increasing of VDW and hydrophobic attractive force, the coal particle changes from kinetically stable to aggregation by increasing HTD from 250 to 300 °C.

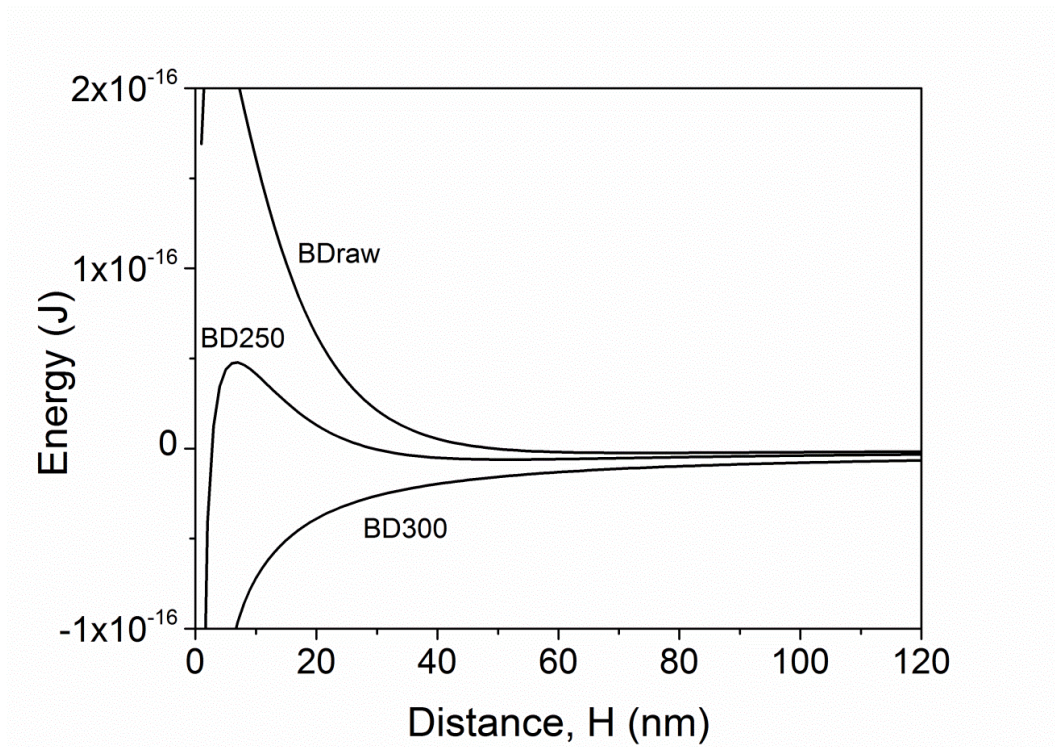


Figure 5.1 Potential energy curves of two coal particles as a function of their distance modeled by extend DLVO theory. Data for numerical calculations are: $a = 40 \mu\text{m}$, $\kappa = 1 \times 10^8 \text{ m}^{-1}$ [73] (Insensitve for the value of V_T in the case of BDraw and BD300), $\epsilon = 7.08 \times 10^{-10} \text{ C}^2/\text{Nm}^2$

5.2 STABILITY

In a dilute colloidal system, the aggregation between particles results in a loss of stability and fast sedimentation. On the contrary, in a heavily loaded suspension (e.g. $> 60 \text{ wt}\%$) with non-colloidal particles, like CWS, the aggregation may prevent particles from settling [44].

The boundary between hard sediment and soft sediment or soft coagulations is obscure, because there is no clear standard to define the hardness of sediments.

Therefore, it is hard to define the static or sediment stability of CWS. In this study, the glass rod penetration tests was applied to measure the hard sediment of CWS, while the mud line measurement was used to verify the phase separation or volume of sediments. A CWS with ideal stability should have a penetration of 100 %, which means no hard sediment, while a separation ratio of 0 % means no sedimentation.

Figure 5.2 shows that the BD300 slurry in both 57.2 and 50 wt% db are stable with a penetration ratio above 92 %, even after 7 days' (168 hours) storage. The coal particles in BD250 and BD raw slurry settle quicker in the first 48 hours and reach plateau of hard sediment at the penetration ratio around 28% and 17 % respectively.

Figure 5.3 shows that both raw and hydrothermally treated slurry have a soft sediment layer between the clear supernatant (dark semi-transparent solution) and sediment (black and opaque phase) as shown in Figure 3.5. The two phases separate quickly in the first 48 hours then reach a plateau.

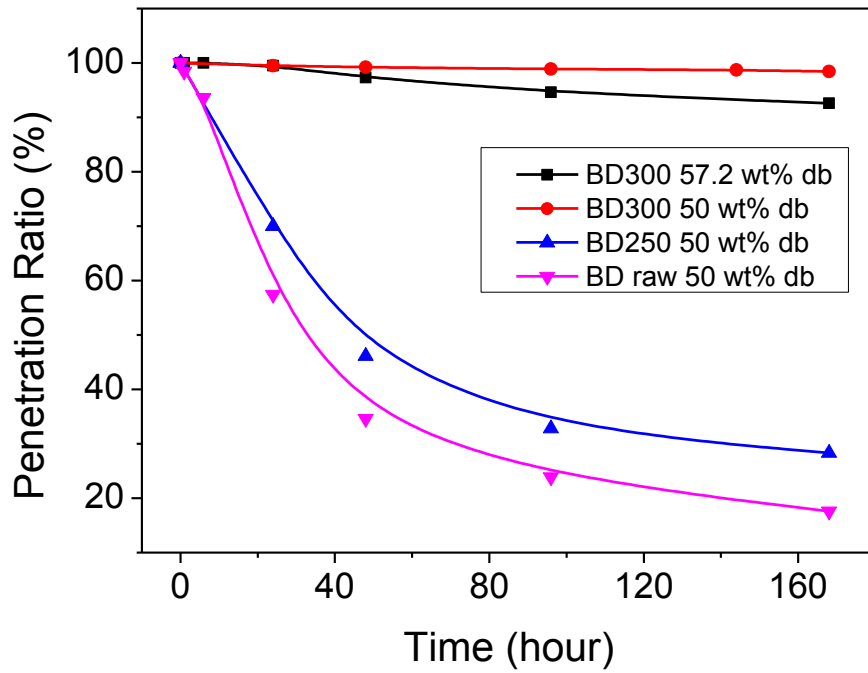


Figure 5.2 Effect of storage time on stability of CWS indicated by penetration ratio

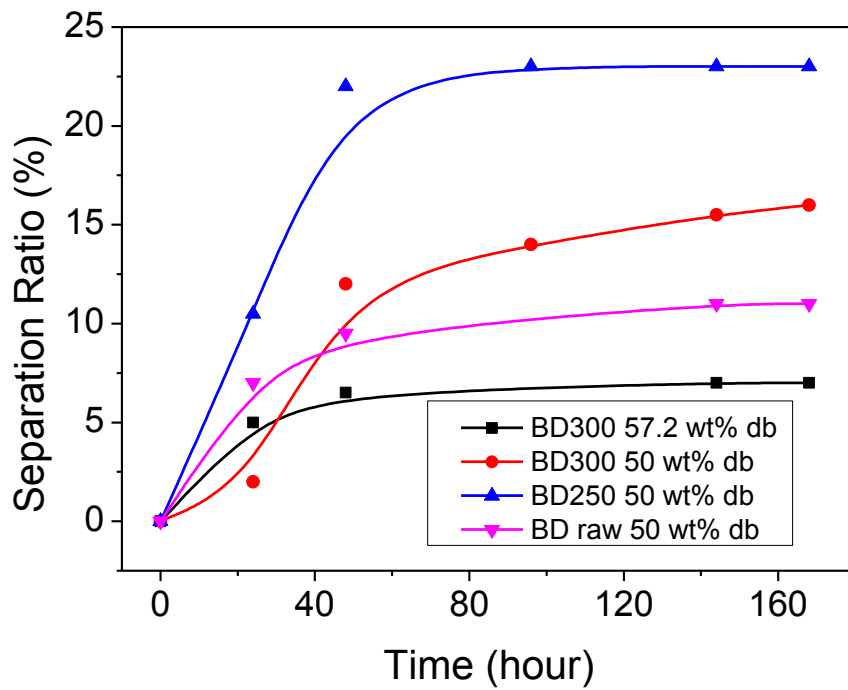


Figure 5.3 Effect of storage time on stability of CWS indicated by separation ratio

5.3 YIELD STRESS AND FRACTAL DIMENSION

The viscosity of raw lignite water slurry has little change and no yield stress is observed over the shear rate range imposed as shown in Figure 5.4. After hydrothermal dewatering, the lignite water slurries exhibit shear-thinning behavior at low shear rate with a yield stress. Herschel-Bulkley (H-B) model [74] which contains both power law function with a yield stress term is widely used to model the fluid exhibit both a yield stress and pseudoplastic behavior as shown in Equation (5-7):

$$\sigma = \sigma_0 + K\dot{\gamma}^n \quad (5 - 7)$$

where σ and σ_0 are shear stress and yield stress (in Pa) respectively; $\dot{\gamma}$ is shear rate (in s^{-1}); n is flow index (dimensionless); K is consistency (in $Pa \cdot s^n$). σ_0 , K and n are fitting parameters shown in the legend of Figure 5.4. Herschel-Bulkley model agrees well with the experimental data. After hydrothermal dewatering the CWS exhibit a yield stress (σ_0) that increases along with temperature of hydrothermal dewatering.

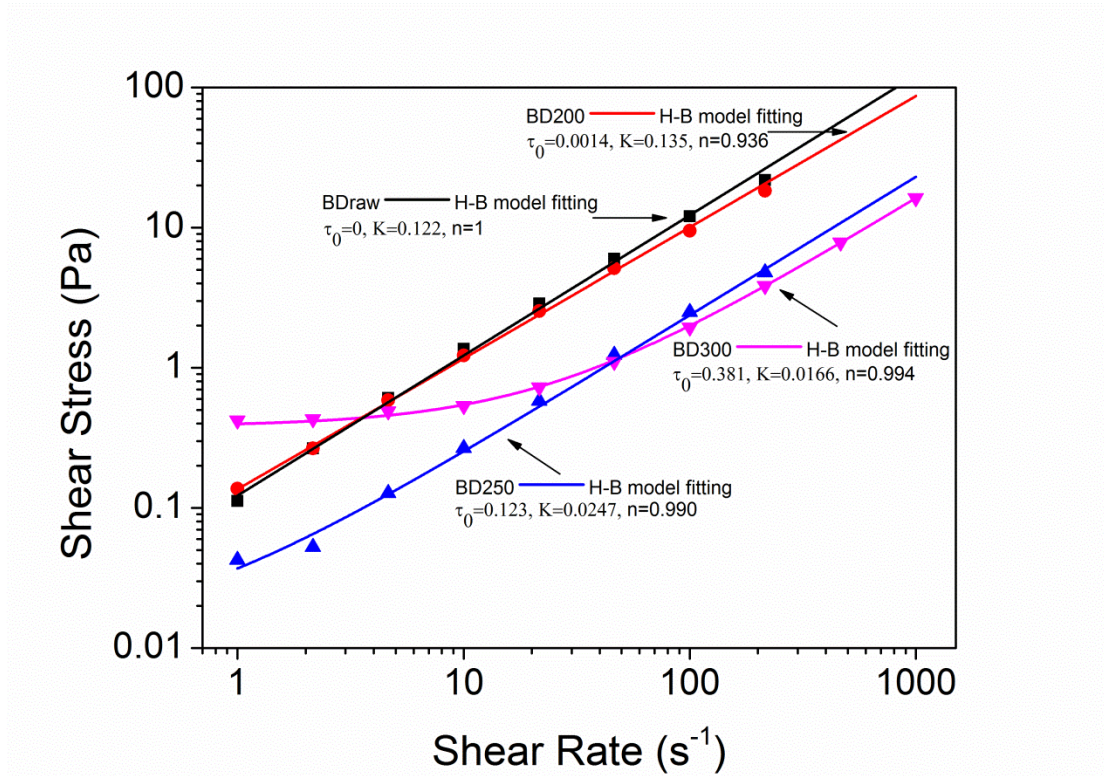


Figure 5.4 Effect of hydrothermal dewatering temperature on the shear stress at different shear rate (samples are all at 45 wt% db)

Liao et al. [75] measured the mass fractal dimension values of coal aggregates by qualitative image analysis, 3D structural analysis, small angle light scattering, light obscuration and settling tests. Due to the assumptions of each measurement, the values of fractal dimensions were not consistent but in an acceptable range. Also, all these method are not in-situ measurement and not suitable for dense CWS. Meanwhile the breakages of aggregation structure are inevitable when transferring samples and during measurement.

In this paper, the fractal dimension of coal aggregations was obtained by employing a scaling law proposed by Dorget [76] shown as below [76]:

$$\sigma_0 \approx \beta \frac{kT R}{a^3 a} (\phi_v)^{4/(3-D)} \quad (5 - 8)$$

where σ_0 is the yield stress; ϕ_v is the particle volume fraction; D is the fractal dimension; k is the Boltzmann constant and T the temperature, a is the radius of a single particle and R is the radius of gyration of the aggregates; β is a coefficient taking account the structural rigidity. When the volume fraction is close to the sol-gel transition, the fractal dimension is close to a constant value and the yield stress follows a power law relation with volume fraction [77-79], based on Equation (5-8) as:

$$\sigma_0 \propto (\phi_v)^{4/(3-D)} \quad (5 - 9)$$

Figure 5.5 shows that the yield stress follows a power law relation with volume fraction. The values of yield stress are obtained from fitting H-B model as illustrated in Figure 5.4. From 38 to 56 volume percent, it follows $\sigma_0 \propto \phi_v^{7.5}$. By applying Equation (5-9), the fractal dimension of BD300 is 2.47. This value is in the range of 2.27–2.66, which was measured by Liao et al. [75] for compact coal aggregates.

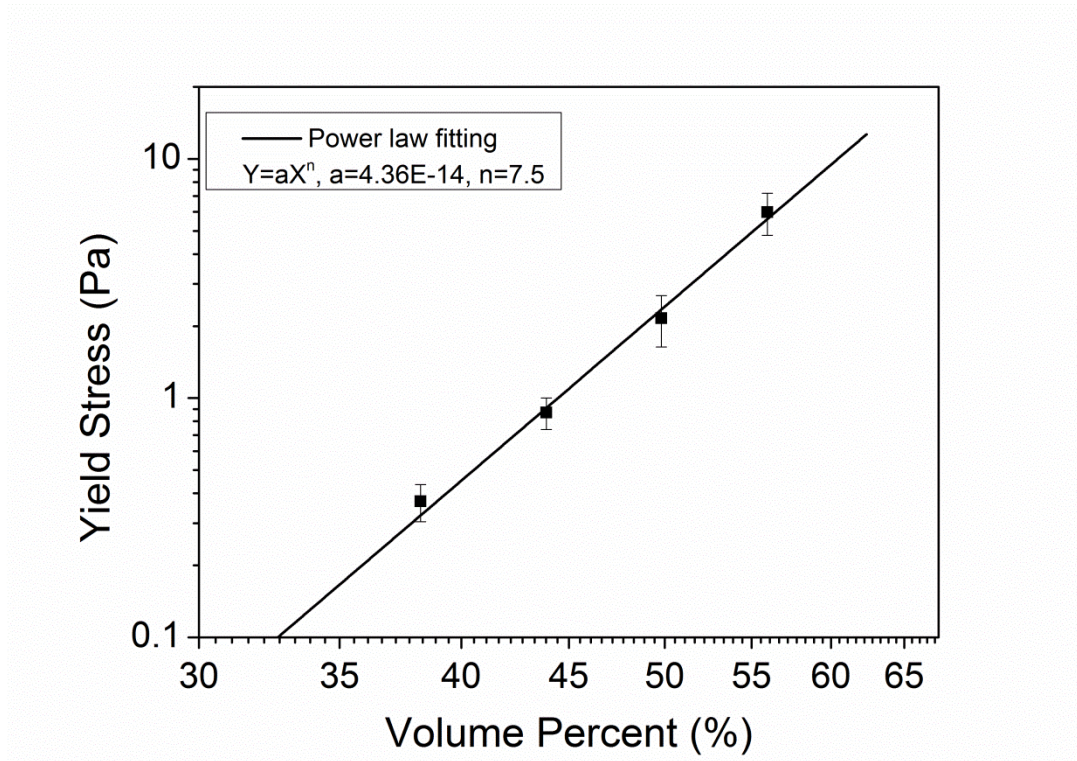


Figure 5.5 Yield stress in relation with volume fraction

6 THE EFFECTS OF HYDROTHERMAL TREATMENT ON THE RHEOLOGICAL BEHAVIORS OF LIGNITE WATER SLURRY

6.1 MEASUREMENT

For a certain type of lignite water slurry, the viscosity (η) depends on the solid loading (φ) or solid volume (ϕ), shear rate ($\dot{\gamma}$) and particle size distribution (ψ), namely $\eta(\varphi, \dot{\gamma}, \psi)$ or $\eta(\phi, \dot{\gamma}, \psi)$. In addition, additives, such as acid/base, electrolytes and polymers, will also affect the viscosity of the slurry

Slurry pumpability is usually measured as the maximum dry solids concentration (φ_{\max}) in slurry with a viscosity of less than 1000 mPa·s at 100 s⁻¹. Before recording the viscosity, a pre-shear and equilibrium time were given to remove the shear history and deliver an equal initial state.

In Figure 6.1, with increasing of shear rate (or shear stress), the microstructure of CWS evolves from State I to State III, namely from strongly aggregation to relative well dispersed [80]. Meanwhile, the energy dissipation is reduced, which shows the decrease of viscosity. Thus, the different behavior of the slurry for high and low shear rates during measurements can be attributed to the different structure development. Meanwhile, with the change of structure the control parameters are different. At low shear rate region (State I), CWS behaves shear

thinning with microstructure rearrangement. The viscosity is influenced mainly by the ratio ϕ/ϕ_m and by non-hydrodynamic parameters, like the particles' shape and their attractive and repulsive forces [81]. For the high shear rate region (State III), CWS behaves more like Newtonian fluid and the viscosity is influenced main by hydrodynamic forces. In intermediate shear rate region (State II), viscosity is influenced by particle-particle interaction and hydrodynamic forces. Because in low shear rate region (State I) the micro-structure is often different in its aggregation states caused by different shear history, the downward is always lower than the upward curve shown the hysteresis or thixotropic of the slurry, as seen in the first figure. While in high shear region (State III), the particles are relatively well dispersed and independent of shear history, dominated by hydrodynamic effects. Therefore, the downward and upward curves are often close, even overlapped in high shear rate region.

In Figure 6.2, three curves are measured independently at increasing shear rate from the same batch and all conditions are the same except pre-shearing. Strong pre-shearing lowers the viscosity at same shear rate. The equilibrium time for micro-structure to recover also affects the viscosity measurement (not shown here). The pre-shear and equilibrium time basically create the same initial condition for every measurement.

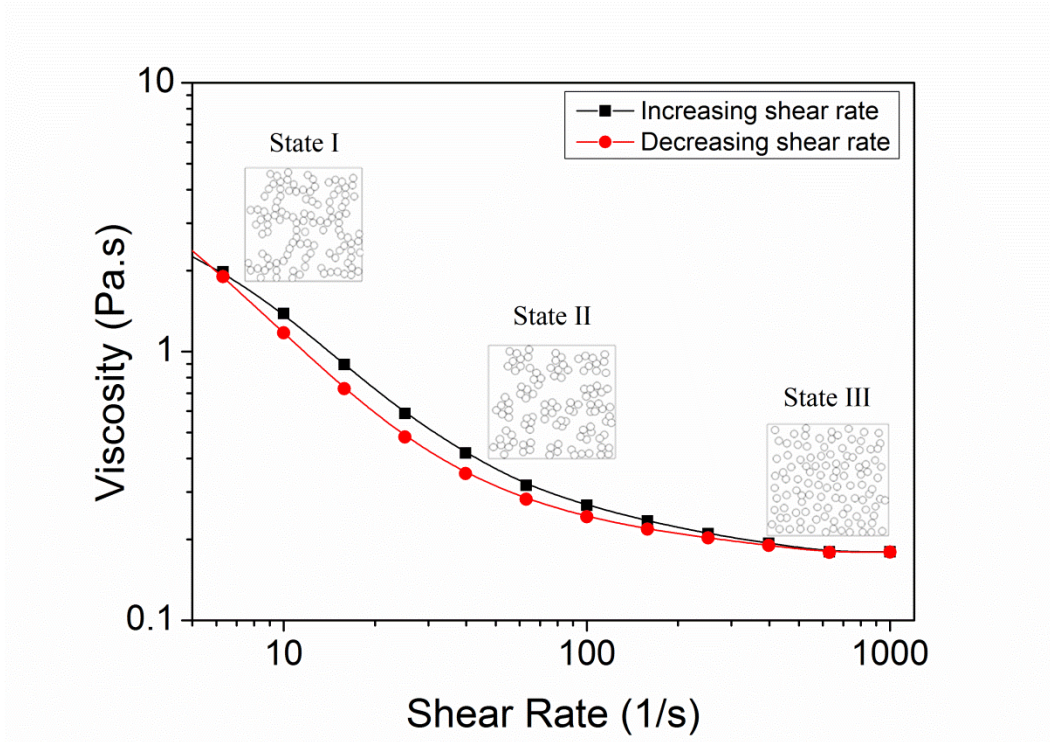


Figure 6.1 Effect of thixotropy on viscosity (sample of BD300 38-75 55wt% db*)

**BD300 38-75 55wt% db means: sample from BD coal processed by hydrothermal dewatering at 300 °C, the particle size range is from 38 to 75 μm , solid concentration is 55% weight percent in dry base. The same is for similar abbreviation.*

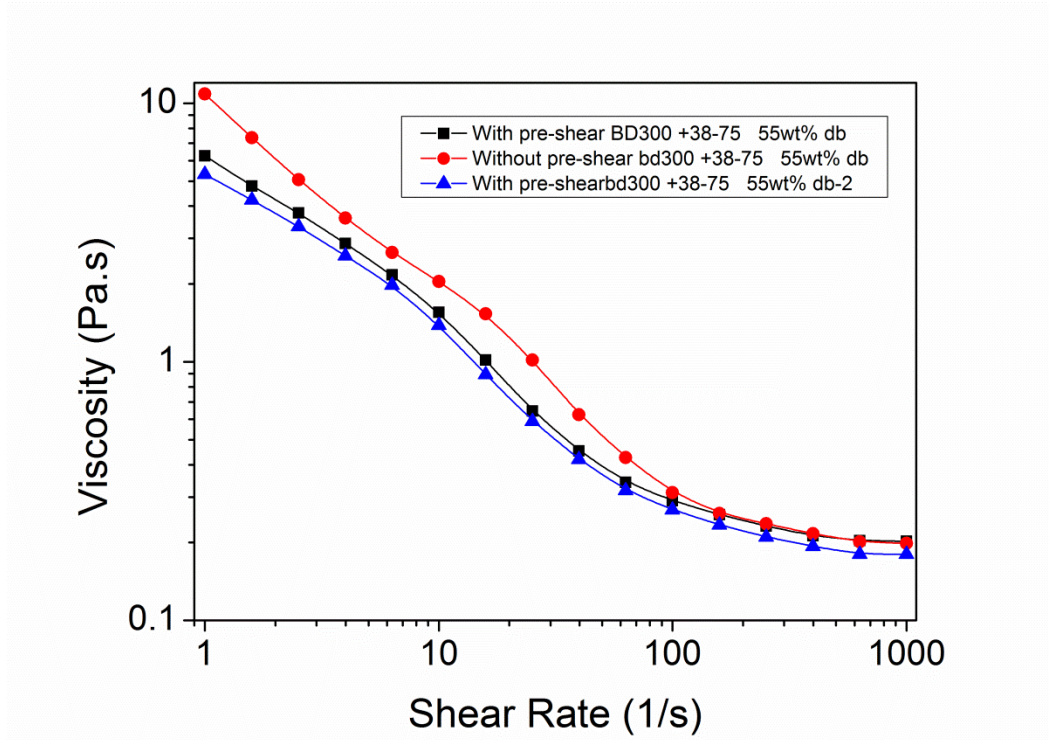


Figure 6.2 Effect of pre-shear on the viscosity (sample of BD300 38-75 55wt% db)

6.2 PARTICLE SIZE DISTRIBUTION

An unimodal coal water slurry may have a maximum solid loading of ~65 wt% where the viscosity becomes infinite, while an idealized multimodal system can generate a theoretically possible solid loading in excess of 80% [32]. However, it is difficult to control the multimodal particle distribution. In our study, we try to maximize the solid loading by using a bimodal distribution. The larger size range used is 106-150 μm , and the smaller size range used is 38-75 μm . The coal samples of both size range is hydrothermally treated at 300 $^{\circ}\text{C}$. In Figure 6.3, it is shown that the viscosity of original CWS can be significantly reduced by mixing

different particle size range. The point of minimum viscosity is at the mixture of 40 wt% of BD 38-75 with 60 wt% of BD 106-150. This is most likely that the finer coal particles fit into the voids of the larger coal particles, forming a higher concentrated package of particles [31]. This optimum particle size distribution will be used for all the rest experiments, except special notice in this chapter.

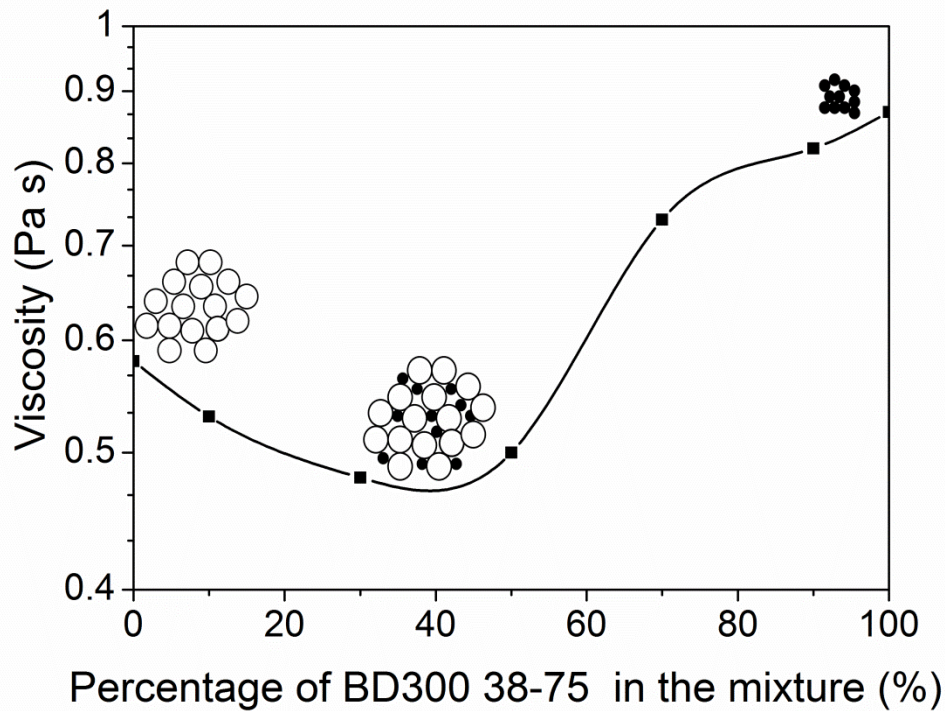


Figure 6.3 Effect of the bimodal particle size distribution on the viscosity of lignite water slurries (58 wt% db total solid loading, mixture combines BD300 38-75 with BD 106-150, 100 s^{-1} shear rate)

6.3 HYDROTHERMAL TREATMENT TEMPERATURE

The viscosity of raw lignite in water slurry without hydrothermal treatment only slightly changed over the shear rate range imposed as shown in Figure 6.4(a).

After hydrothermal dewatering, the lignite water slurries exhibit shear-thinning behavior at low shear rate, and the degree of shear thinning increases with the increase of hydrothermal dewatering temperature. At high shear rate range, e.g., 500-1000 s⁻¹ for BD 300, the Newtonian flow dominates due to the alignment of particles into the flow direction [42]. Sisko model [82] which contains both power law function with shear rate and infinite shear rate viscosity (η_{inf}) is widely used to model the shear rate dependent viscometry as shown in Eqn. (6-1).

$$\eta = \eta_{inf} + k(\dot{\gamma})^{n-1} \quad (6 - 1)$$

where η is the shear viscosity and η_{inf} is the viscosity at "infinity" shear rate; k and n are the consistency coefficient and flow behavior index of the Sisko model. Sisko model is shown to agree well with the experimental data in Figure 6.4 (a). The degree of shear thinning, indicated by n, is found to increase with hydrothermal dewatering temperature. The infinite shear viscosity decreases but the low shear viscosity increases with the increases of hydrothermal treatment temperature. At low shear rate, the increased viscosity is probably due to the increased surface attractive forces between particles [44]. At high shear rate regime, the hydrodynamic force dominates the surface forces. The lower infinite shear viscosity of HTD coal water slurry compared with raw coal water slurry is

most likely because of the smaller effective volume fraction of the HTD coal particle in the slurry, caused by the removal of water inside of coal.

The viscosity of lignite water slurry at 100 s^{-1} shear rate as the function of HTD temperature decreases slightly when the HTD temperature is lower than $200 \text{ }^\circ\text{C}$ as shown in Figure 6.4 (b). A significant decrease in the viscosity of lignite water slurry occurs when HTD temperature reaches $250 \text{ }^\circ\text{C}$. As the stability of the slurry increases with the increase of HTD temperature (visual comparison, data not shown), $300 \text{ }^\circ\text{C}$ is chosen as the optimal HTD temperature to make high solid lignite water slurry.

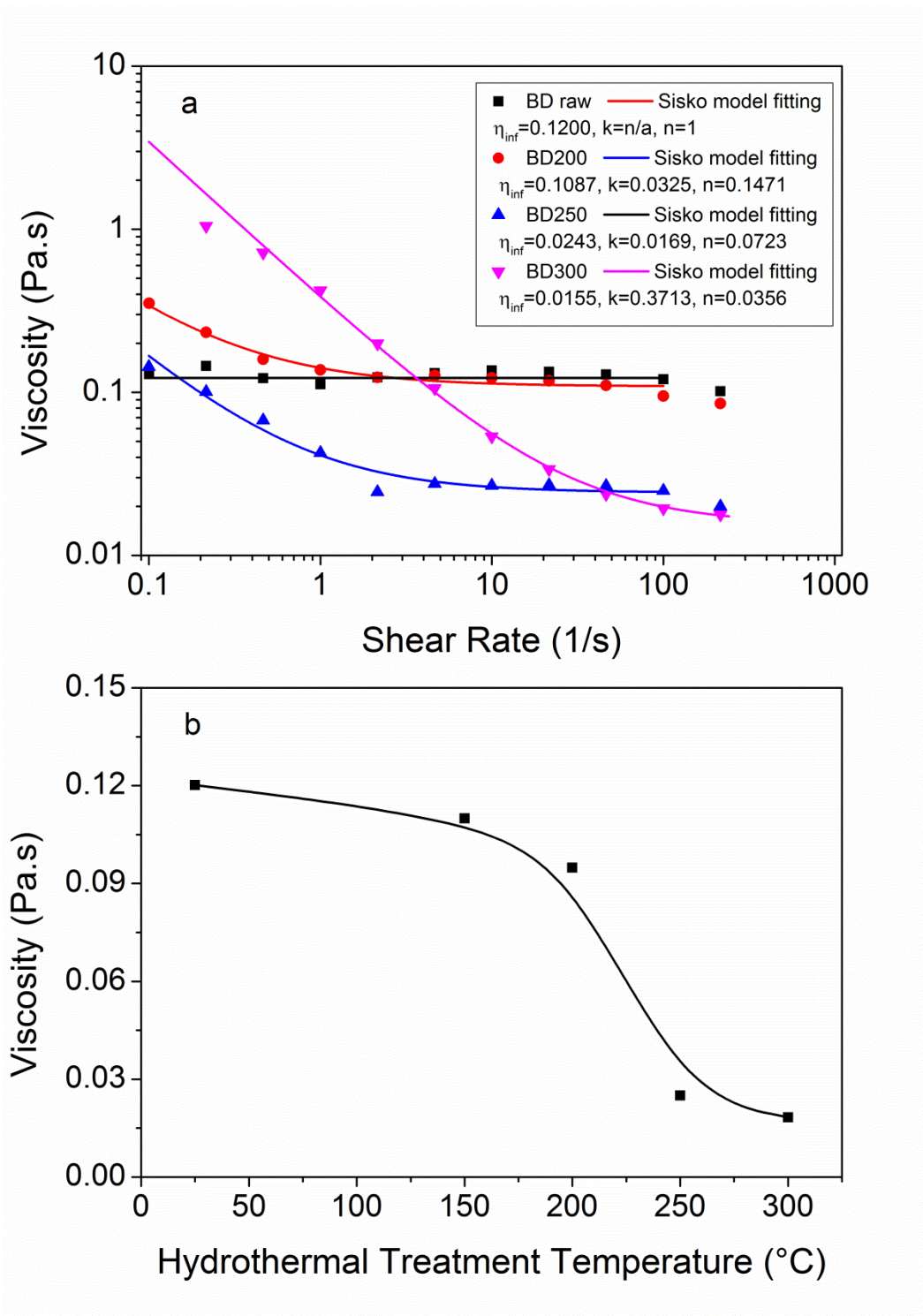


Figure 6.4 Effect of HTD temperature on the viscosity of lignite water slurry. (a) Flow curves at various HTD temperatures; (b) Viscosity at 100 s⁻¹ shear rate versus HTD temperature (45 wt% db lignite water slurry)

6.4 FINES IN CWS

In Figure 6.5, the particle size distribution without fines is generated by wet sieving and the particle size distribution with fines is generated by dry sieving. The particle size distribution of each sample can be seen in Figure 3.3. The curve of dry sieving sample with fines shows more like a shear thinning behavior with a tendency to be Newtonian at high shear rate. While the curve of particle without fines is more like a Newtonian behavior. The fines is more likely to generates microstructure and networks which renders the fluid shear thinning behavior when breaking the microstructure and networks at low shear region. In this way the fines decide the flow types of the slurry. While for the sample without fines, the slurry containing only large particle is more like a hard sphere system. The attraction and repulsion force between large particles (eg. $> 10 \mu\text{m}$) can be neglected and the hydrodynamic force is dominated. Therefore, the sample without fines has lower viscosity in the low shear rate region and higher viscosity in the high shear region.

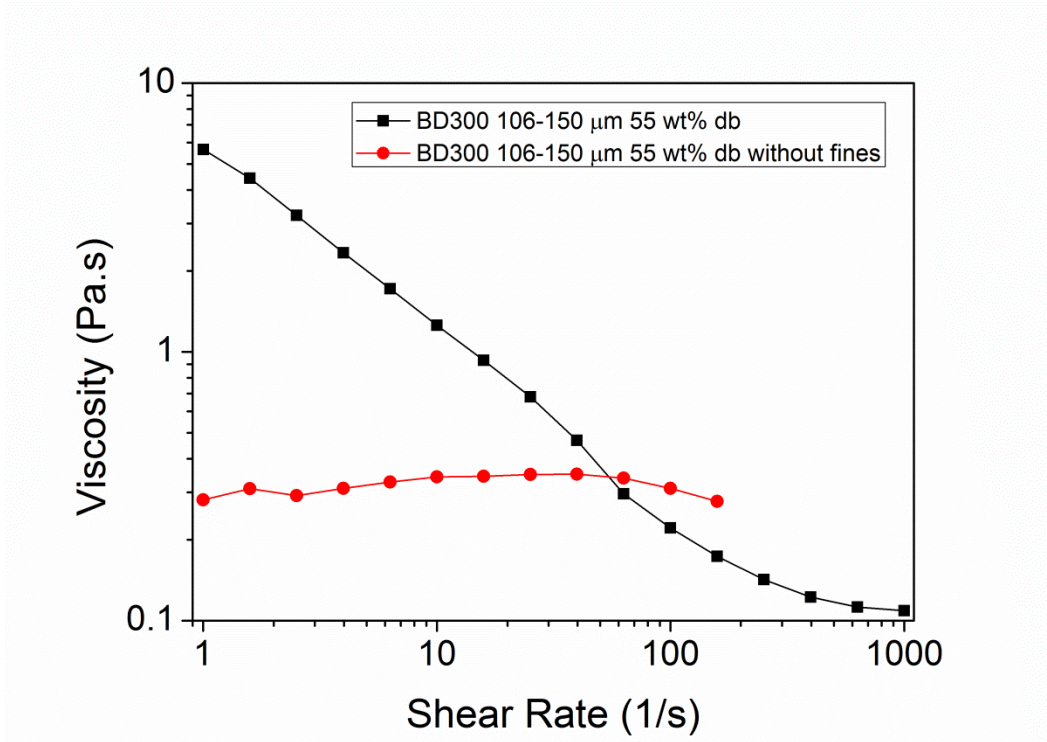


Figure 6.5 Effect of fines on the viscosity of CWS

6.5 VOLUME FRACTION AND MODELING

In this section, a quantitative relationship between the shear viscosity and the solid content will be established. Models of solid content dependent shear viscosity are mostly based on the volume fraction of particles [29, 34, 52]. When converting the solid loading weight percent to solid volume fraction (ϕ), the inherent moisture of lignite should be considered, and the following expression is generally used [34, 36, 52]:

$$\phi = \frac{V_{\text{coal}} + V_{\text{hum}}}{V_{\text{coal}} + V_{\text{H}_2\text{O}}} = \frac{1 + a_{\text{hum}} \left(\frac{\rho_{\text{lignite}}}{\rho_{\text{H}_2\text{O}}} \right)}{1 + \left(\frac{\rho_{\text{lignite}}}{\rho_{\text{H}_2\text{O}}} \right) \left(\frac{m_{\text{H}_2\text{O}}}{m_{\text{lignite}}} \right)} \quad (6 - 2)$$

where V_{coal} , V_{hum} and $V_{\text{H}_2\text{O}}$ are the volume of dry coal, inherent moisture of coal and total water in the slurry respectively; ρ_{lignite} and $\rho_{\text{H}_2\text{O}}$ are the density of dry lignite and water; m_{lignite} and $m_{\text{H}_2\text{O}}$ are the weight of dry lignite and total water in the slurry. In this chapter, the inherent moisture (a_{hum}) of lignite in the slurry equals the summation of the bound water and non-freezable water as stated in Table 4.4. Figure 6.6 shows that at the same solid loading, the volume fraction of raw coal sample is much higher than the volume fraction of the same sample after hydrothermal dewatering at 300 °C. The density of raw coal after hydrothermal dewatering increases from 1.31 to 1.53 g/cm³, which contributes to decreasing the volume of coal particle. The major factor that lowering the volume fraction is the reduction of inherent moisture by the hydrothermal dewatering as illustrated in Figure 6.6.

Figure 6.7 shows the relationship between relative viscosity (η_r) and volume fraction (ϕ). The relative viscosity is gained by dividing apparent viscosity (η) of slurry to the viscosity of solvent (η_0). The relative viscosity increases with increasing of volume fraction. The Krieger-Dougherty (K-D) rheological model [83] is often used to correlate η_r , and ϕ :

$$\eta_r = [1 - (\phi/\phi_{\text{max}})]^{-[\eta]\phi_{\text{max}}} \quad (6 - 3)$$

where $[\eta]$ is the intrinsic viscosity (dimensionless) and ϕ_{\max} is the maximum solid volume fraction (dimensionless). The intrinsic viscosity $[\eta]$ strongly depends on the particle shape [29, 34, 52, 84]. For example, the intrinsic viscosity of sphere is 2.5, while for cubic, it is around 3.1 [85]. The maximum solid loading ϕ_{\max} is strongly dependent on the particle size distribution and shear rate. For example, the maximum solid volume for uniform hard spheres theoretically ranges from 0.67 to 0.74, but for idealized multimodal system, the maximum solid volume fraction can exceed 0.8 [44]. In Figure 6.7 experimental data of both raw and hydrothermal treated slurries are fitted using Eqn. (6-3). The intrinsic viscosity increases due to the hydrothermal treatment. The maximum solid volumes of both raw and HTD coal samples are around 0.72.

In Figure 6.7, the relative viscosity of raw CWS is shown to be lower than hydrothermal dewatered CWS at the same volume fraction. Hydrothermal dewatering can increase the attractive forces between particles, which will increase the dissipation energy of fluid, thus increase the viscosity at same volume fraction. However, compared with Figure 6.6, the relative viscosity of raw coal CWS is higher than hydrothermal dewatered CWS at the same solid loading. This difference of relative viscosity when converting solid loading to volume fraction is caused mainly by reduction of inherent moisture along with increasing the

density by hydrothermal dewatering as illustrated in Figure 6.6. In the solid loading - viscosity figure, the influence of reducing inherent moisture and increasing coal density dominates the influence of increasing surface attractive forces on viscosity of slurry. This reveals the nature that by reducing the inherent moisture and increase the density of lignite, HTD increases solid loading of lignite water slurry.

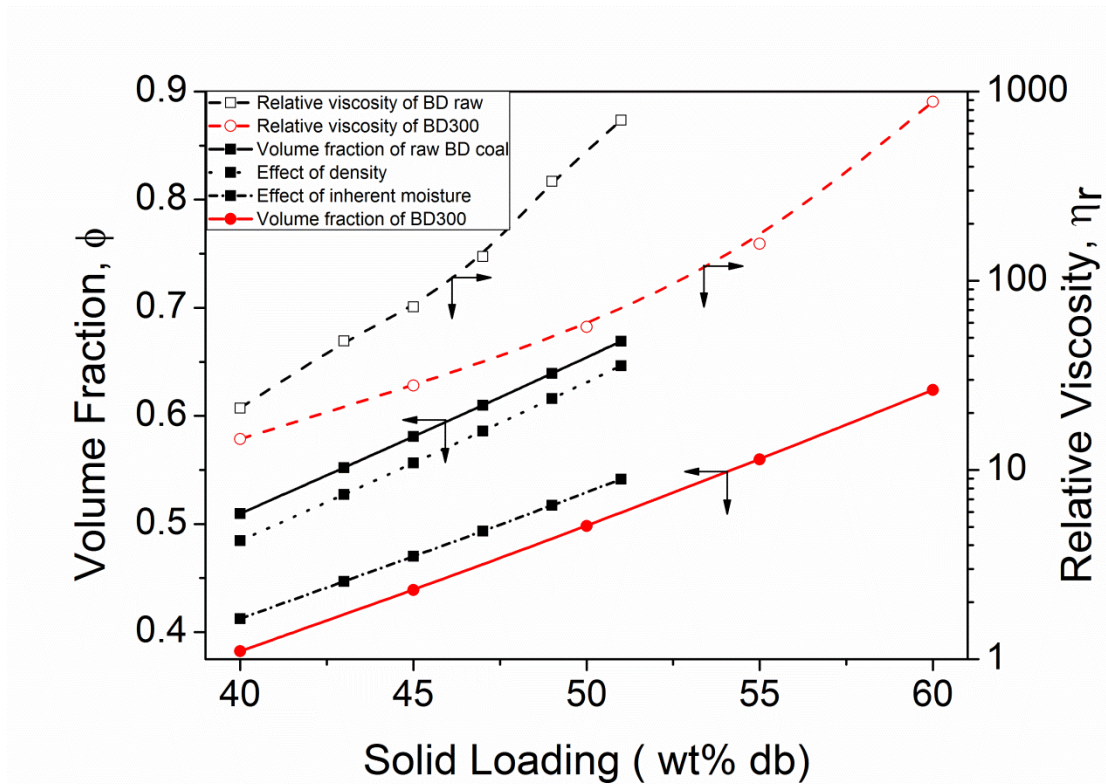


Figure 6.6 Conversion of solid loading to volume fraction and the relation with relative viscosity (at 100 s^{-1})

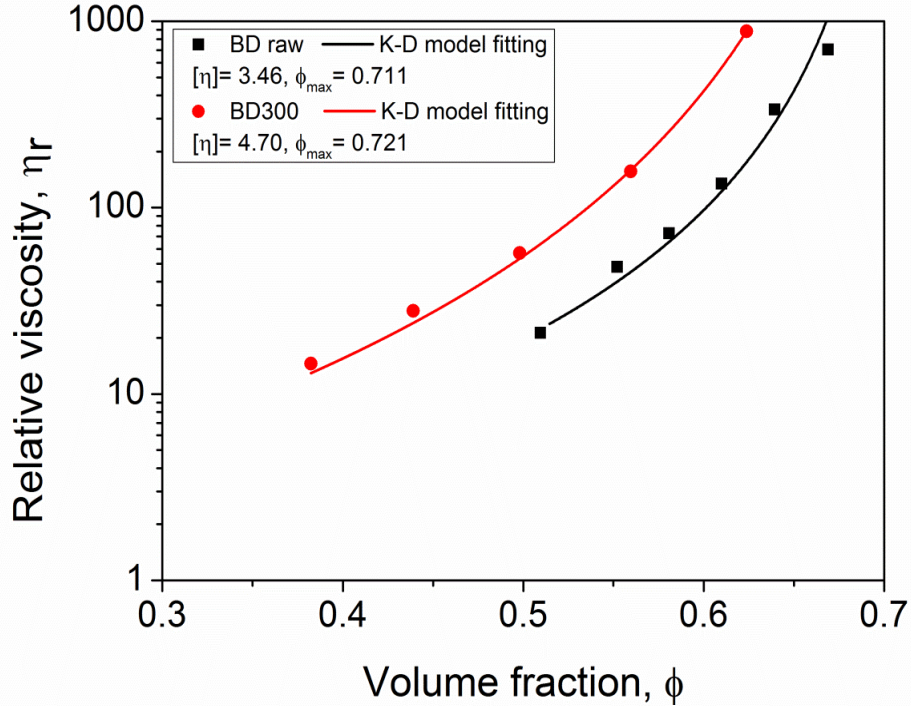


Figure 6.7 Effect of volume fraction on the relative viscosity of raw and HTD lignite water slurry (at 100 s^{-1})

6.6 DISPERSANT

Polycarboxylic ether (PCE) used in this study is a comb-type polymer consisting of a sodium polymethacrylate backbone and polyethylene-oxide (PEO) side chains, as described by Zhang et al. [86]. The PEO side chains adsorbed on hydrophilic site of coal [87, 88] and the dispersant creates electrostatic and steric repulsive force by negatively charged carboxylate groups on the backbone and highly hydrated PEO side chains [86] as illustrated in Figure 6.8.

Figure 6.9 shows the effect of the concentration of PCE on the viscosity of raw and HTD CWS at 100 s^{-1} . The viscosity of raw CWS increases with adding

dispersant. The viscosity of CWS with hydrothermal treatment at 300 °C increases initially and then decreases after 0.5 wt% dosage, at last slight increase again. The viscosity of both slurries increases initially due to the bridge effect that PCE (molecular weight around 40,000 Dalton) may link the coal particles together. As illustrated in Figure 6.8, for the CWS made by BD300 coal, the dispersants break the aggregation by increase electrostatic and steric repulsive force, thus decreasing the viscosity. While for the CWS made by raw BD coal, the coal particles are already well dispersed due to the hydrophilic surfaces between coal particles [44], adding dispersants in raw lignite water slurry may only slightly decrease the viscosity. Finally, the viscosity of both slurries increases again due to the volume of the slurry is occupied by the excessively added PCE. For example, if the D_{50} of coal particles is 40 μm and the size of PCE molecule is 10 nm, then by adding 1 wt% PCE, the volume occupied by PCE will be around 2 percents of the total volume, as illustrated by the calculation in the Appendix 2.

Figure 6.10 shows that the maximum dry solid loading of raw coal slurry is around 50 wt% db. After the hydrothermal treatment, the maximum dry solid loading increases to around 57 wt% db and further increases to around 60 wt% db by optimizing particle size distribution as shown in Figure 6.3. The maximum dry solid loading increases to 62 wt% db by adding 1 wt % of polycarboxylate ether

dispersant. The solid lines, as shown in Figure 8, are the fittings using equation (6-4) which is based on Equation (6-2) and Equation (6-3).

$$\eta = \left(\frac{100/\varphi - 1 - a_{\text{hum}}}{100/\varphi - 1 + \rho_{\text{solvent}}/\rho_{\text{coal}}} \right)^{-[\eta]\phi_{\text{max}}} * \eta_0 \quad (6 - 4)$$

where η and η_0 are the viscosity of slurry and solvent respectively; ρ_{solvent} and ρ_{coal} are the density of solvent (here is water) and dry coal respectively; a_{hum} is inherent moisture of coal (for high rank coal, this value is close to zero); $[\eta]$ and ϕ_{max} is the intrinsic viscosity (dimensionless) and maximum solid volume fraction (dimensionless) and can be acquired from fitting the experiment data or measurement.

In Figure 6.10, the fitting parameter of intrinsic viscosity ($[\eta]$) is the same for HTD CWS with different particle size and distribution. Intrinsic viscosity $[\eta]$ depends strongly on the particle shape [29, 34, 52, 84]. The CWS with different size and distribution, after hydrothermal dewatering at 300 °C, may have the same particle shape change from raw coal [89] and similar aggregating pattern, which creating a similar value of intrinsic viscosity. While the maximum solid volume fraction (ϕ_{max}) is strongly dependent on the particle size distribution at the shear rate of 100 s⁻¹. ϕ_{max} of HTD300 Mixture is greater than that of HTD300 106-150

μm and HTD300 38-75 μm . After adding enough dispersant (1 wt% for HTD300), the aggregates of coal particles is dispersed, resulting in a higher ϕ_{max} .

Eqn. (6-4) is found to agree with the experiment data well. By applying the derived Krieger-Dougherty model, the viscosity of coal water slurry as a function of solid weight percentage can be predicted with limited experiment data, especially at high solid loading where the viscosity is hard to be measured correctly.

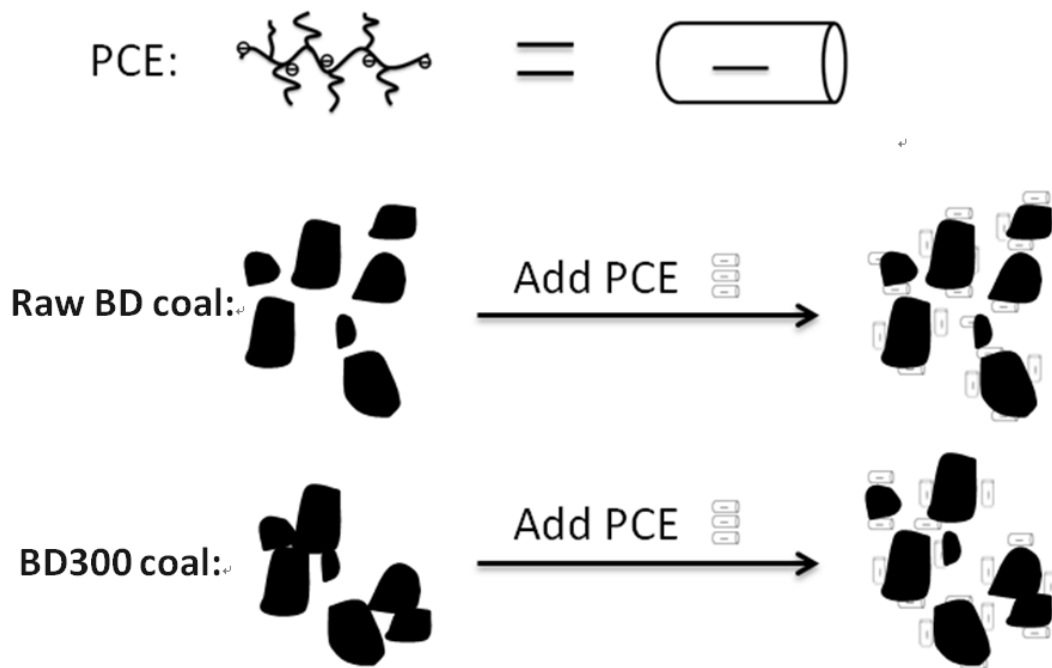


Figure 6.8 Illustrations on the interactions between different coal particles and PCE molecules

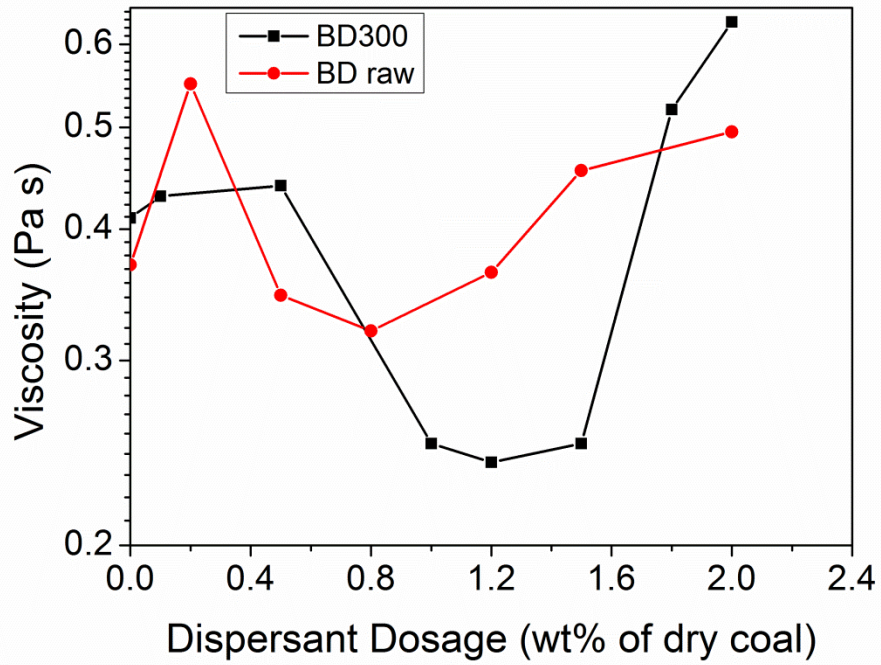


Figure 6.9 Effect of dispersant concentration on the viscosity of coal water slurries.
(Sample: BD300 slurry 58 wt% db, BD raw slurry 48 wt% db, pH= 7.5 ± 0.5)

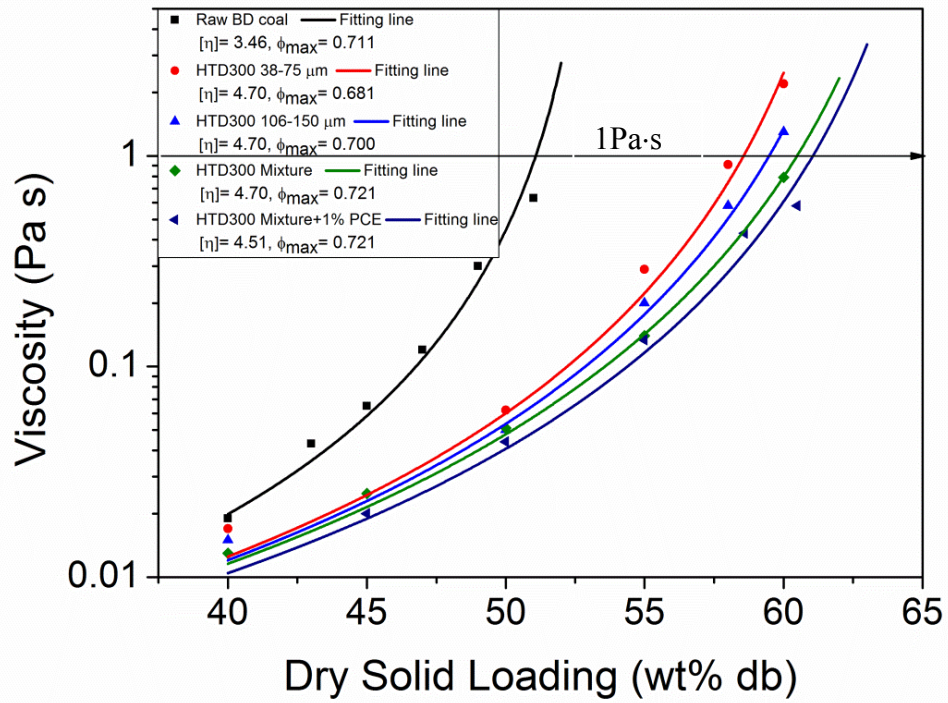


Figure 6.10 Effect of hydrothermal treatment, particle size distribution and dispersant on the viscosity of lignite water slurry (at 100 s^{-1})

7. CONCLUSIONS

The hydrothermal dewatering of lignite for making high solid loading and stable slurry was investigated in this research. The experimental work includes three main parts: i) the effects of hydrothermal treatment on bulk and surface properties of lignite; ii) the effects of hydrothermal treatment on the stability of lignite water slurry; iii) the effects of hydrothermal treatment on the rheological behaviors of lignite water slurry. The main conclusions are:

1. Hydrothermal treatment can significantly reduce the moisture and increase the fixed carbon content of lignite and heating value. It can efficiently prevent moisture re-absorption from 30-35 wt% db to 10-15 wt% db (at relative vapor pressure of 96%, 30 °C) after hydrothermal treatment at 300 °C.
2. More oxygen functional group was decomposed associated with increasing the temperature hydrothermal treatment, which was shown by the decrease of their characteristic peaks in DRIFTS and the change of zeta potential. The surfaces of lignite become more hydrophobic, as shown by contact angle measurement. The contact angle is increased from ca. 60° to ca. 90° after hydrothermal treatment. The increase of surface hydrophobicity is attributed to the decomposition of oxygen functional group and surface covering of tar leached during hydrothermal treatment.
3. The zeta potential becomes less negative after HTD, probably due to the decomposition of oxygen functional group. The increased surface hydrophobicity could promote coal particle hydrophobic attractions.

4. When the temperature of wet BD coal decreases, two exothermal peaks (ca. -12 °C and ca. -40 °C) were found in DSC graph. The non-freezable water was found not to freeze even at -90 °C.
5. More than half of the non-freezable water and bound water can be removed by hydrothermal treatment at 300 °C, as indicated in the DSC method. The amount of non-freezable water and bound water is slightly higher than the equilibrium moisture, measured at 96 % relative vapour pressure and 30 °C. The former amount is more close to inherent moisture and is used to calculate the volume fraction of coal particles in slurry.
6. Hydrothermal treatment increases the attractive forces between coal particles by modifying the surface properties of coal, which is modeled by extended DLVO theory with parameters from contact angle and zeta potential measurement.
7. Lignite water slurry after HTD becomes more stable as shown by the stability measurements. The fractal dimension of lignite water slurry after HTD at 300 °C is 2.47, which indicates that the slurry formed an aggregate network to prevent the coal particles from settling.
8. The reliable measurement of rheology of lignite water slurry is developed by adding proper pre-shearing and equilibrium time. The hydrothermally treated lignite water slurry behaves shear-thinning in the range of 1 s^{-1} to 1000 s^{-1} while viscosity of raw lignite slurry changes slightly at this range. The shear rate - viscosity curve was fitted by Sisko model with a good agreement.
9. The viscosity of lignite water slurry can be significantly reduced by hydrothermal treatment when the temperature is over 200 °C. Increasing the temperature of hydrothermal treatment (<320 °C) will lower the viscosity.

10. It is proposed that by permanently reducing the inherent moisture along with increasing coal density the hydrothermal dewatering increases the solid loading of lignite water slurry.
11. By hydrothermal treatment at 300 °C, particle size mixing and adding 1% PCE dispersant, the maximum solids concentration of lignite water slurry can reach as high as 62 wt% db.

8. CONTRIBUTION TO ORIGINAL KNOWLEDGE

The following two major contributions to the literature are achieved.

1. The effect of HTD on the stability of CWS.

Hydrothermal treatment increases the attractive forces between coal particles, leading to the aggregation of coal particle across whole slurry system. The aggregation network of coal particles was proposed to prevent the coal particles from settling.

2. The effect of HTD on the rheological properties and maximum solid loading of CWS.

Hydrothermal treatment decreases the inherent moisture and increase true density of coal particles permanently. This will reduce the volume fraction of coal particles in slurry, compared with the raw lignite slurry at same dry solid loading. Therefore, at same dry solid loading due to the lower volume fraction, HTD treated lignite water slurry shows a lower viscosity.

9. FUTURE WORK

The following suggestions are recommended for future research:

1. Build a database combining the parameters of hydrothermal dewatering temperature, particle size mixing and energy consumption to predict the maximum solids concentration in each condition for further industrialization.
2. Develop a bench-scale system of continuous hydrothermal treatment system, evolving from batch reaction of autoclave to continuous reaction, closer to industrial and commercial application.
3. Screen and synthesize more efficient dispersant to reduce the viscosity of hydrothermal treated lignite water slurry. Understand the interaction between dispersant and coal particle. The effect of organic content released in slurry by HTD needs to be investigated.
4. Investigate the rheology of HTD lignite water slurry during pipeline transportation and atomization in nozzle during combustion and gasification.

REFERENCES

- [1] BP p.l.c., BP Statistical Review of World Energy, London, United Kingdom, June 2010.
- [2] World Energy Council - Survey of Energy Resources 2010.
- [3] Karthikeyan, Muthusamy, Wu Zhonghua, and Arun S. Mujumdar. "Low-rank coal drying technologies—Current status and new developments." *Drying Technology* 27.3 (2009): 403-415.
- [4] Fleissner, H. (1927) 'Method of drying coal and the like', Patent No. US1632829.
- [5] Fleissner, H. (1927) 'Method of drying coal and the like', Patent No. US1632829.
- [6] Favas, G.; Jackson, W. R. "Hydrothermal dewatering of lower rank coals. 2. Effects of coal characteristics for a range of Australian and international coals" *Fuel* 2003, 82, 59–69.
- [7] AP Burdukov, VI Popov, VG Tomilov and VD Fedosenko, "The rheodynamics and combustion of coal-water mixtures," *Fuel*, vol.81, pp.927-933, 2002.
- [8] Moriyama, Ryo, et al. "Upgrading of low rank coal as coal water slurry and its utilization." *Coal Preparation* 25.4 (2005): 193-210.
- [9] Favas, G., Jackson, W. R., & Marshall, M. (2003). "Hydrothermal dewatering of lower rank coals. 3. High-concentration slurries from hydrothermally treated lower rank coals." *Fuel*, 82 (1), 71-79.
- [10] Hodges S, Woskoboenko F. 9th International Conference on Coal Research, Washington, USA (1993)
- [11] Exergen CHTD (continuous Hydrothermal dewatering) technology. <http://www.all-energy.com.au/userfiles/file/Jack-Hamilton-121011.pdf>. Oct. 10, 2012
- [12] RWE (Rhenish-Westphalian Electric) WTA technology. <http://www.rwe.com/web/cms/contentblob/2978/data/8744/DL-WTA-Technology.pdf>. Oct. 10, 2012
- [13] Drycol process patented by DBA Global. <http://drycol.com/index.html>. Oct. 10, 2012
- [14] Evans, D. G., and Siemon, S. R. (1970) "Dewatering of brown coal before combustion." *Journal of the Institute of Fuel*, 43, 413-419.
- [15] Evans, D. G., and Siemon, S. R. (1970) 'Separation of water from solid organic materials', Patent No. AU 430626.
- [16] Evans, D. G., and Siemon, S. R. (1971) 'The separation of water from solid organic materials', Patent No. US 3552031.

- [17] Murray, J. B., and Evans, D. G. (1972) "The brown-coal/water system: Part 3. Thermal dewatering of brown coal." *Fuel*, 51, 290-296.
- [18] Okuma, O., Inoue, T., Yasumuro, M., Shindo, A., Hirano, T., and Matsumura, T. "Hydrothermal pretreatment of Victorian brown coal for liquefaction", 3rd Japan/Australian Joint Technical Meeting on Coal, Brisbane, Australia. 1993.
- [19] Jantao Zhao, Moshfiqur Rahman, Qingxia Liu, Ling Zhang, Rajender Gupta, "Effect of Hydrothermal Treatment on the Low Rank Coal Flotation", *Prepr. Pap.-Am. Chem. Soc., Div. Fuel Chem.* 2012, 57 (1), 205-206.
- [20] Inoue, T.; Okuma, O.; Masuda, K.; Yasumuro, M.; Miura, K., "Hydrothermal treatment of brown coal to improve the space time yield of a direct liquefaction reactor." *Energy & Fuels* 26.4 (2012): 2198-2203.
- [21] Lee, S., Speight, J. G., & Loyalka, S. K. (Eds.). (2007). *Handbook of alternative fuel technologies*. crc Press. [chapter 4].
- [22] Kesavan, S., *Stabilization of Coal Particle Suspensions using Coal Liquids*, M.S. thesis, University of Akron, 1985.
- [23] Papachristodoulou, G. and Trass, O., "Coal slurry fuel technology", *Can. J. Chem. Eng.*, 65, 177–201, 1987.
- [24] SMITH, HERBERT R. "Improvement in Liquid Fuels." U.S. Patent No. 219,181. 2 Sep. 1879.
- [25] Kawatra, S.K., *Coal-water slurries*, in *Encyclopedia of Chemical Processing*, Lee, S., Ed., Vol. 1, Taylor & Francis, New York, 2005, pp. 495–503.
- [26] Broilick, H. I. "Innovative Transport Modes Coal Slurry Pipelines." *Proceedings of the 15th International Conference on Coal and Slurry Technologies*, Florida, the United States. 1990.
- [27] Kawatra, S.K. and Bakshi, A.K., "The on-line pressure vessel rheometer for concentrated coal slurries", *Coal Prep.*, 22(1), 2002.
- [28] Manford, R.K., "Coal-water slurry: a status report", *Energy*, 11, 11/12, 1157–1162, 1986.
- [29] Goudoulas, T. B., Kastrinakis, E. G., & Nychas, S. G. (2003). "Rheological aspects of dense lignite-water suspensions; time dependence, preshear and solids loading effects". *Rheologica acta*, 42(1-2), 73-85.
- [30] Barnes, H.A., Hutton, J.F., and Walters, K., *An Introduction to Rheology*, Elsevier, New York, 1989.
- [31] Yavuz, R., and S. Küçükbayrak. "Effect of particle size distribution on rheology of lignite-water slurry." *Energy sources* 20.9 (1998): 787-794.

- [32] Hunter, R.J., *Foundations of Colloidal Science*, Vol. 1, Oxford University Press, Oxford, 1987.
- [33] Rowell, R. L. "THE CINDERELLA SYN-FUEL-FIND JOY IN SLURRIES." *Chemtech* 19.4 (1989): 244-248.
- [34] Roh, N.-S., Shin, D.-H., Kim, D.-C., and Kim, J.-D., "Rheological behavior of coal-water mixtures 1. Effects of coal type, loading and particle size", *Fuel*, 74, 8, 1220–1225, 1995.
- [35] Woskoboenko, F., Siemon, S.R., and Creasy, D.E., "Rheology of Victorian brown coal slurries, 1. Raw coal-water", *Fuel*, 66, 1299–1304, September 1987.
- [36] Kaji, R., Muranaka, Y., Miyadera, H., and Hishinuma, Y., "Effect of electrolyte on the rheological properties of coal-water mixtures", *AIChE J.*, 33, 1, 11–18, 1987.
- [37] Rowell, R.L., Vasconcellos, S.R., Sala, R.J., and Farinato, R.S., "Coal-oil mixtures 2. Surfactant effectiveness on coal oil mixture stability with a sedimentation column", *Ind. Eng. Chem., Proc. Des. Dev.*, 20, 283–288, 1981.
- [38] Johnson, Stephen B., et al. "Surface chemistry–rheology relationships in concentrated mineral suspensions." *International Journal of Mineral Processing* 58.1 (2000): 267-304.
- [39] Napper, D.H., *Polymeric Stabilization of Colloidal Dispersions*, Academic Press, 1983.
- [40] Gregory, J., *Flocculation of polymers and polyelectrolytes*, *Solid Liquid Dispersions*, Tadros, T.F., Ed., Academic Press, pp. 163–181, 1987.
- [41] Evans, D.F. and Wennerstrom, H., *The Colloidal Domain Where Physics, Chemistry, Biology, and Technology Meet*, VCH, New York, 1994.
- [42] Mewis, J., & Wagner, N. J. (2012). *Colloidal suspension rheology*. Cambridge University Press.
- [43] IUPAC. *Compendium of Chemical Terminology*, 2nd ed. (the "Gold Book"). Compiled by A. D. McNaught and A. Wilkinson. Blackwell Scientific Publications, Oxford (1997). XML on-line corrected version: <http://goldbook.iupac.org/W06691.html>.
- [44] Laskowski, J.S. *Coal flotation and fine coal utilization*; Elsevier: Amsterdam, 2001. [Chapter 10]
- [45] J.S. Laskowski and G.D. Parfitt, *Electrokinetics of coal-water slurry*. In: G.D. Bostsaris and Y.M. Glazman (eds), *Interfacial Phenomena in Coal Technology*. Marcel Dekker, New York, 1989, p. 322.
- [46] Turian, R.M., Fakhreddine, M.K., Avramidis, K.S., and Sung, D.-J., "Yield stress of coal-water mixtures", *Fuel*, 72, 9, 1305–1315, 1993.

- [47] Potas, Todd A., et al. "Preparation of hydrothermally treated LRC/water fuel slurries." *Chemical Engineering Communications* 44.1-6 (1986): 133-151.
- [48] Suwono, Aryadi, and Hamdani. "Upgrading the Indonesian's low rank coal by superheated steam drying with tar coating process and its application for preparation of CWM." *Coal Perparation* 21.1 (1999): 149-159.
- [49] H Usui, T Tatsukawa, T Saeki, K Katagiri, "Upgrading of low rank coal by a combined process of vacuum drying and tar coating." *Coal Perparation* 21.1 (1999): 71-81.
- [50] Yu, Yujie, et al. "Effect of hydrothermal dewatering on the slurryability of brown coals." *Energy Conversion and Management* 57 (2012): 8-12.
- [51] Guo, Jian. Hydrothermal-mechanical dewatering of brown coal. PhD diss. Monash University. Faculty of Engineering. Department of Chemical Engineering, 2000.
- [52] Goudoulas, Thomas B., Eleftherios G. Kastrinakis, and Stavros G. Nychas. "Preparation and Rheological Characterization of Lignite– Water Slurries." *Energy & Fuels* 24.1 (2009): 496-502.
- [53] ASTM D1412-07, 2007, Standard test method for equilibrium moisture of coal at 96 to 97% relative humidity and 30°C: ASTM International. West Conshohocken, PA, 2007, DOI: 10.1520/D1412-07. www.astm.org.
- [54] Norinaga, Koyo, et al. "Classification of water sorbed in coal on the basis of congelation characteristics." *Energy & fuels* 12.3 (1998): 574-579.
- [55] Fei, Yi, et al. "Lignite–water interactions studied by phase transition — differential scanning calorimetry." *Fuel* 84.12 (2005): 1557-1562.
- [56] Qiu, Xueqing, et al. "Evaluation of sulphonated acetone–formaldehyde (SAF) used in coal water slurries prepared from different coals." *Fuel* 86.10 (2007): 1439-1445.
- [57] Speight, James G. *Handbook of coal analysis*. Vol. 166. John Wiley & Sons, 2005.
- [58] Parikh, Jigisha, S. A. Channiwala, and G. K. Ghosal. "A correlation for calculating HHV from proximate analysis of solid fuels." *Fuel* 84.5 (2005): 487-494.
- [59] Hayashi, Jun-ichiro, et al. "Estimation of size and shape of pores in moist coal utilizing sorbed water as a molecular probe." *Energy & fuels* 15.4 (2001): 903-909.
- [60] Mraw, Stephen C., and Deborah F. O'Rourke. "Water in coal pores: The enthalpy of fusion reflects pore size distribution." *Journal of Colloid and Interface Science* 89.1 (1982): 268-271.

- [61] Landry, Michael R. "Thermoporometry by differential scanning calorimetry: experimental considerations and applications." *Thermochimica acta* 433.1 (2005): 27-50.
- [62] Norinaga, Koyo, et al. "Evaluation of effect of predrying on the porous structure of water-swollen coal based on the freezing property of pore condensed water." *Energy & fuels* 13.5 (1999): 1058-1066.
- [63] He, Y. B., and J. S. Laskowski. "Contact angle measurements on discs compressed from fine coal." *Coal Preparation* 10.1-4 (1992): 19-36.
- [64] ANDREAS GEORGAKOPOULOS, *Energy Sources*, 25:995–1005, 2003.
- [65] Wang, Yonggang, et al. "Impacts of inherent O-containing functional groups on the surface properties of Shengli lignite." *Energy & Fuels* 28.2 (2014): 862-867.
- [66] Xu, Zhenghe, and Roe-Hoan Yoon. "The role of hydrophobia interactions in coagulation." *Journal of Colloid and Interface Science* 132.2 (1989): 532-541.
- [67] Berg, John C. *An introduction to interfaces & colloids: the bridge to nanoscience*. World Scientific, 2010.
- [68] Rabinovich, Y., Churaev, N V, 1979. "Effect of electromagnetic delay on the forces of molecular attraction", *Kolloidnyi Zhurnal*, 41:468-474.
- [69] Yoon, Roe-Hoan, Darrin H. Flinn, and Yakov I. Rabinovich. "Hydrophobic interactions between dissimilar surfaces." *Journal of colloid and interface science* 185.2 (1997): 363-370.
- [70] Pazhianur, R., and R-H. Yoon. "Model for the origin of hydrophobic force." *Minerals & metallurgical processing* 20.4 (2003): 178-184.
- [71] Soni, Gaurav. *Development and Validation of a Simulator based on a First-Principle Flotation Model*. PhD Diss. Virginia Polytechnic Institute and State University, 2013.
- [72] Chaturvedi, Tanmay, J. M. Schembre, and A. R. Kavscek. "Spontaneous imbibition and wettability characteristics of Powder River Basin coal." *International Journal of Coal Geology* 77.1 (2009): 34-42.
- [73] Biletsky, V., P. Sergeyev, and O. Krut. "Fundamentals of highly loaded coal-water slurries." *Mining of Mineral Deposits*. Ed. Pivnyak, Genadiy, et al.. London: CRC Press, 2013. 105-113.
- [74] Herschel, W.H.; Bulkley, R. (1926), "Konsistenzmessungen von Gummi-Benzollösungen", *Kolloid Zeitschrift* 39: 291–300.
- [75] Liao, Jimmy YH, et al. "On different approaches to estimate the mass fractal dimension of coal aggregates." *Particle & Particle Systems Characterization* 22.5 (2005): 299-309.
- [76] M. Dorget, Ph.D. thesis, Institute National Polytechnique, Grenoble, France, 1995.

- [77] Pignon, Frédéric, Jean-Michel Piau, and Albert Magnin. "Structure and pertinent length scale of a discotic clay gel." *Physical review letters* 76.25 (1996): 4857.
- [78] Pignon, Frédéric, et al. "Yield stress thixotropic clay suspension: Investigations of structure by light, neutron, and x-ray scattering." *Physical Review E* 56.3 (1997): 3281.
- [79] Piau, J. M., M. Dorget, and J. F. Paliarne. "Shear elasticity and yield stress of silica-silicone physical gels: Fractal approach." *Journal of Rheology* 43.2 (1999): 305-314.
- [80] Wildemuth, C. R., and M. C. Williams. "A new interpretation of viscosity and yield stress in dense slurries: coal and other irregular particles." *Rheologica Acta* 24.1 (1985): 75-91.
- [81] Boyle, F., H. Dincer, and G. Ateşok. "Effect of coal particle size distribution, volume fraction and rank on the rheology of coal-water slurries." *Fuel Processing Technology* 85.4 (2004): 241-250.
- [82] Sisko, A. W. "The flow of lubricating greases." *Industrial & Engineering Chemistry* 50.12 (1958): 1789-1792.
- [83] Krieger, Irvin M. "Rheology of monodisperse latices." *Advances in Colloid and Interface Science* 3.2 (1972): 111-136..
- [84] Usui, Hiromoto. "A thixotropy model for coal-water mixtures." *Journal of non-newtonian fluid mechanics* 60.2 (1995): 259-275.
- [85] Mallavajula, Rajesh K., Donald L. Koch, and Lynden A. Archer. "Intrinsic viscosity of a suspension of cubes." *Physical Review E* 88.5 (2013): 052302.
- [86] Zhang, Ling, et al. "Effect of polycarboxylate ether comb-type polymer on viscosity and interfacial properties of kaolinite clay suspensions." *Journal of colloid and interface science* 378.1 (2012): 222-231.
- [87] E Taylor, W. Liang, G. Bognolo and Th.E Tadros, "Concentrated coal-water suspensions containing non-ionic surfactants and polyelectrolytes." *Coll. Surf.*, 61 (1991) 147.
- [88] S. Chander, B.R. Mohal and EE Aplan, "Wetting behavior of coal in the presence of some nonionic surfactants." *Coll. Surf.*, 26 (1987) 205.
- [89] Karayıldırım, Tamer, A. Sınağ, and Andrea Kruse. "Char and coke formation as unwanted side reaction of the hydrothermal biomass gasification." *Chemical engineering & technology* 31.11 (2008): 1561-1568.

APPENDIX

A.1 ENERGY BALANCE OF HTD AND COMPARISON WITH THERMAL DRYING

In this part, the theoretical calculation of energy consumption between traditional thermal drying and hydrothermal dewatering is demonstrated.

Major assumptions:

- The energy required is divided into: 1) Raising Temperature.; 2) Keeping temperature.; 3) heat loss.
- The temperature of reactor surface is constant at 50 0C. Heat loss of other part is neglected.
- The heat capacity of the dry coal is constant. Water content of coal is 60%. In HTD process, the coal water ratio is 1 : 1 and the water doesn't evaporate.
- In thermal drying, the temperature rises from 20 0C to 105 0C for half hour. The temperature keeps at 105 0C for 1 hour and finally cools down naturally . The final water content of treated coal is 5 %.

- When recycling heat from HTD, there is a heat loss at 50 °C and 10 % water loss.

Major parameters and values used for calculation are listed in Table A.1.

Table A.1 Parameters used for calculation

Parameter	Description	Value	Unit
h	Heat transfer coefficient	2.71	$W/(m^2\text{°C})$
A	Surface area of heat bath	0.33	m^2
C_p	Specific heat capacity of coal	1.6	$kJ/(kg\text{°C})$
$C_{p(\text{dried coal})}$	Weight of coal	1.3	$kJ/(kg\text{°C})$
m_{coal}	Weight of coal	0.05	kg
M_{moisture}	Weight of moisture	0.013	kg
T_{∞}	Ambient temperature	20	°C
H_v	Heat of evaporation	2260	kJ/kg
T_{surface}	Temperature of heat bath	50	°C

Major equation used in the calculation:

1. Calculating energy for increasing temperature of water:

$$Q_1 = m_{\text{water}} \int_{T_1}^{T_2} C_{p \text{ water}} dT \quad (\text{A} - 1)$$

$$C_{p \text{ water}} = A + BT + CT^2 + DT^3 + ET^4 \quad (\text{A} - 2)$$

2. Calculating energy required for evaporating moisture from coal

$$Q_2 = m_{\text{moisture}} h_v \quad (\text{A} - 3)$$

3. Calculating energy for increasing temperature of coal:

$$Q_2 = m_{\text{coal}} C_p \Delta T \quad (\text{A} - 4)$$

4. Calculating heat loss:

$$\frac{dQ_2}{dt} = hA (T - T_{\infty}) \quad (\text{A} - 5)$$

$$\rightarrow Q_2 = \int_0^t hA (T_{\text{surface}} - T_{\infty}) dt \quad (\text{A} - 6)$$

The results of calculation are illustrated in Figure A.1. From Figure A.1, it shows that:

1. HTD with heat recycle consumes less energy than thermal drying.
2. Coal water ratio affects the energy for HTD, while coal's water content has minor effects on it.
3. The water content of coal strongly affects the energy efficiency for thermal drying.

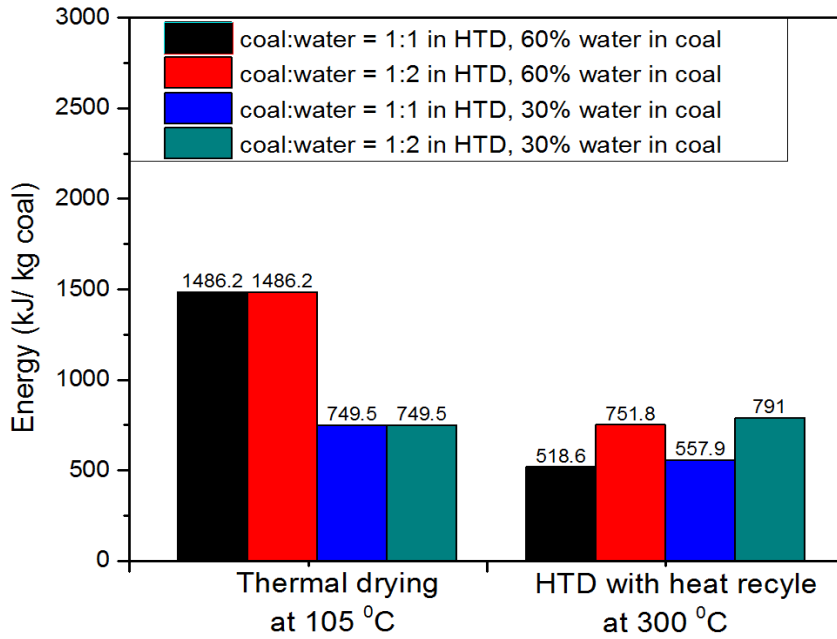


Figure A.1 Comparison of HTD and thermal drying at different initial water contents in coal samples

From the above figure, the energy consumption of ideal CHTD with heat recycle is less than traditional thermal drying. Except energy consumption, other characteristics are compared below.

- **Safety:** HTD is relative safe because it is operated in a water environment. While thermal drying needs special care about safety issue, due to the spontaneous combustion and explosion of lignite [3].
- **Moisture reabsorption:** lignite after HTD has a good resistance to moisture reabsorption [6]. After thermal drying, lignite is easy for moisture reabsorption.

- **Final moisture:** after HTD lignite still needs further drying, such as filtration and vacuum drying. In thermal drying process, the moisture in lignite can be dried directly below 10%.
- **Making CWS:** after HTD lignite has a good slurryability, up to around 62% solid concentration [9]. The slurryability of thermally dried lignite is nearly not improved.

A.2 CALCULATION OF PCE VOLUME PERCENT

Table A.1 shows the main values and parameters for this calculation. We assume that volume of the slurry (V_t) is 100 ml for calculation.

Table A.2 Parameters and values for PCE volume percent calculation

	BDraw
Coal weight percent, w_c (wt% db)	48
PCE weight percent of coal, w_p (vol%)	1
True density (g/cm^3)	1.31
Slurry density, ρ_s (g/ml)	1.13
Molecular Weight of PCE, MW (Dalton)	40000
Avogadro constant, N_A (mol^{-1})	6.02×10^{23}
The length of single PCE molecule, D , (nm)	10

The equations used for calculating the volume percent of PEC in slurry (vol%) are listed below.

$$m_p = V_t \rho_s w_c w_p \quad (A - 7)$$

$$N = \frac{m_p}{MW} N_A \quad (A - 8)$$

$$V_0 = \frac{4}{3} \pi \left(\frac{D}{2}\right)^3 \quad (A - 9)$$

$$\text{vol}\% = \frac{NV_0}{V_t} \quad (A - 10)$$

V_0 is the volume of single PCE molecule and N is the number of PCE molecule.

By calculation with the equations above and the values in Table A.1, if adding 1 wt% PCE, the volume occupied by PCE will be around 2 percents of the total volume (vol % = 2).